Cloudrider Aircraft Concept

Team
Balázs Nagy
Soma Detre

Academic Support and Advisiors
Institute of Aircraft Design, TU Munich
Univ. Prof. Dr.- Ing. Mirko Hornung
Lysandros Anastasopoulos

Lehrstuhl für Luftfahrtsysteme

Table of contents

List of Figures:

List of Tables:

Nomenclature

ACN	Aircraft Classification Number
Alt	Altitude
BACS	Bleed Air Cooling System
BPR	Bypass Ratio
CCS	Cryogenic Cooling System
CE	Combustion Engine
COC	Cash Operating Cost
COSAR	Cost Specific Air Range
CROR	Contra-Rotating Open Rotor
DEP	Distributed Electric Propulsion
DHPS	Double-Hybrid Propulsion System
DMC	Direct Maintenance Costs
DoH	Degree-of-Hybridization
DP	Distributed Propulsion
EASAR	Energy Specific Air Range
EC	European Commission
EF	Electro Fan
EIS	Entry-into-Service
EROPS	Extended Range Operations
ETOPS	Extended Range Operation with Two-Engine Airplanes
ETS	Emission Trading System

FAA	Federal Aviation Administration
FoM	Figure-of-Merit
FoM	Figure-of-merit
HLFC	Hybrid Laminar Flow Control
HTS	High-Temperature-Superconducting
ICAO	International Civil Aviation Organization
ISA	International Standard Atmosphere
ITB	Inter-stage Turbine Burner
ITB EF	Inter-stage Turbine Burner Energy Fraction
LFL	Landing Field Length
LHV	Lower Heating Value
LNG	Liquid Natural Gas
LTO	Landing and Take Off
MFHE	Multi-Fuel Hybrid Engine
MTOW	Maximum Take Off Weight
NLF	Natural Laminar Flow
HNLC	Hybrid Natural Laminar Flow Control
OEI	One Engine Inoperative
OR	Open Rotor
OWE	Overall Weight Empty
PAX	Passenger
PCN	Pavement Classification Number
ROC	Rate of Climb
PrP	Prandtl Plane
SEP	Specific Excess Power
SSPC	Surface Superconducting Photocurrent
ST	Superconducting Temperature
USB	Upper Surface Blowing
TAS	True Airspeed
TF	Turbo Fan
TLAR	Top Level Aircraft Requirements
TOC	Top of Climb
TOFL	Take Off Field Length
TSFC	Thrust Specific Fuel Consumption
TSPC	Thrust Specific Power Consumption

Abstract

This project aims to identify future market and technology trends after that introduce a non-conventional, ultra-efficient aircraft design, which follows these and also complies with new NASA N+3 [9markt] and European Union Flightpath 2050 [10markt] requirements, especially focusing on the energy reduction and the alternative propulsion and energy systems.

In this design study, within the framework of the Aircraft Design Challenge of the NASA and DLR will be a unique design and a novel propulsion system with three different energy sources investigated and implemented, in order to fulfil the strict requirements for the future aircraft design. The four main part of the design process are the analysis of the market demand, the aerodynamics, propulsion system and the investigation of feasibility with the help of comparison to the baseline aircrafts.

The aerodynamic design of the Cloudrider concept has a semi conventional, three lifting surface with a promising total wetted area reduction potential. To maximize the aerodynamic efficiency, high aspect ratio wings are deployed, equipped with hybrid laminar flow control (HLFC) devices.

The non-regular hybrid-distributed-propulsion system with three different energy sources has many design challenges during the sizing process and also need a novel handling process solution. These challenges include, among others the engine optimization, which was conducted in the flexible modeling environment CycleTempo®. To achieve the prescribed energy reduction the operating mode of the gas turbine and the batteries was also investigated simulated based on in-house developed model implemented in Wolfram Mathematica®. In addition, with regards to motive power the proposal utilizes ducted fans run by High-Temperature Super-conducting (HTS) electric motors.

The resulting optimized propulsion system combined with the novel airframe design of the Cloudrider concept had achieved 85% in total LTO NOx and 60.6% reduction in energy in payload km compared to the Boeing B737-900ER baseline aircraft.

1 Introduction

A large airport with a high volume of passengers carrying their luggage, going through the checking gates, boarding different airplanes, taxiing on the runway, hearing the shrill of the turbines and then go and reach your faraway destination within a few hours. Since the middle of the XX. Century this has been the ordinary routine for more and more people every day. The aviation industry has grown huge, and it is still growing. Future analysis shows that the number of flights will double [1] by 2030 (relative to 2011). There is still clearly an enormous economic potential in aviation [2]. But there are other factors too, the planet is getting warmer, the sea is rising, and our world is changing, people are becoming more conscious and eco-friendly. Therefore, to maintain a sustainable market growth, and keep our planet for the future generations, consideration of environmental and social effects during the design process of future airplanes will be crucial. Objectives for new N+3 vision of the NASA target is a more than 60% fuel-burn, 80% NOx and 75% CO_2 reductions compared to the year 2000 [3]. Even more ambitious goals outlined in Flightpath 2050 [4] by the European Commission (EC) for the year 2050 is a 75% reduction in CO2-emissions per passenger kilometer (PAX km) relative to the capabilities of conventional aircraft of the year 2000. Furthermore, a 90% reduction of NOx-emissions and a 65% perceived noise reduction is advocated. Finally, aircraft movements on the ground have to be emission-free when taxiing [4].

This project is based around a concept called the Cloudrider, which combines a unique design and a novel propulsion system of alternative fuels. This project aims to identify future market and technology trends after that introduce a non-conventional, ultra-efficient aircraft design, which follows these and also complies with new NASA N+3 [3] and European Commission Flightpath 2050 [4] requirements. The Entry-into-Service (EIS) for the Cloudrider concept is set as 2045. After the introduction of the main results of aerodynamics and propulsion system design process a feasibility analysis is performed as well.

„SINE PENNIS VOLARE HAUD FACILE EST."

[Titus Maccius Plautus]

2 Future trends and Market Assessment

Within the next three decades, due to the cost of jet fuel and the increasing number of aircraft flying every day, the world of aviation will have to cope with more stringent environmental constraints and traffic density increase.

Aviation industry has done its share to reduce the emissions and today's modern airliners are 70% more efficient than they were 40 years ago and they reduced their NOx, CO and HC emissions as well [5]. However, this reduction trend must continue to fulfil the noise, 60% fuel-burn, 80% NOx and 75% CO_2 reduction prescribed from NASA and the European Commission compared to the year 2005. Similar to this, the aircraft movements on the ground have to be emission-free when taxiing [4].Technologies which meet these targets will significantly reduce carbon and noise footprints from aviation.

Therefore, in undertaking a comprehensive interdisciplinary design and integration project, we focused on an integrated alternative energy propulsion system in order to establish the best means to provide energy for the aircraft to reduce its footprint and fuel consumption.

A novel propulsion system is considered to be a key enabler in achieving these challenging targets. Partially responsible for present achievements is the Distributed Electric Propulsion (DEP) technology, which has been applied for different aircraft configurations (such as the N+3 Aircraft generation from NASA [6]). Results show a drag reduction (which leads to lower fuel consumption) and also a better efficiency due to the aero propulsive effects [7].

In addition, the introduction of super-conducting technologies in electric motors promises a dramatic improvement in power-specific weights, whose application in the aviation industry was investigated intensively by both EU and US research institutions [8]. However, the future development of this technology has to solve the weight penalty derived from the cryogenic cooling system, which is also a target of the Cloudrider concept.

Since the energy crisis in 1973 there have been concerted efforts to conserve fuel due to its rising cost [5]. Similar to this, an important consideration is the scarcity of crude oil in the coming years, thus adding another dimension to the major challenges facing future design and product development of aircraft [9]. This tendency led to the investigation of aircraft concepts using alternative energy sources [10]. On the other hand, wing design characteristics have since changed to become more fuel efficient [5]. Due to this design consideration, the wing aspect ratio is being increased on some existing aircraft, which increases the wingspan by 6 to 7% [5], which will probably lead to the change of the ICAO Annex 14 Code C limitation (now 36.0 m box) regulations [5].

The global growth in commercial aviation is estimated to be 4.8% per year in passenger traffic and 4.2% in freight traffic over the next twenty years [2]. 63% of cargo aircraft are converted or designed from passenger aircraft platforms. Therefore, the passenger aircraft needs to be convertible and equipped with proper cargo loading facilities [5].

Due to the new type of energy sources with the hybrid aircraft, a major challenge for the aviation industry is the reduction of turnaround times by 40% by 2050 using novel handling concepts [10]. According to [10], in order to achieve a lower cost and energy of a hybrid aircraft propulsion system significant changes in optimal conditions with respect to altitude and speed may occur.

In the future, aviation will be likely affected by new technologies and development trends in other industrial fields. Fostered by the progress made in the automotive industry, aeronautics took an interest in hybrid propulsion and battery technology [7].

Over the next 20 years 38% of aircrafts delivery demand is expected to come from Asian and 21% from the North America region [11]. 40% of the fuel consumption in aviation is derived from the large single-aisle airlines [2]. Consequently, to meet the market requirement a large passenger capacity above 250 seats and a minimum range of 6000 km is recommended for an economical realizable concept. Deriving these global trends and demands the Cloudrider is specified for a range of 7000 km (3780 nm), seats of 300 PAX and a cruise speed of Mach 0.75, which is also necessary for the integration into the air traffic of the future.

3 The Cloudrider concept

3.1 Airframe

Based on literature research (exposed in 4.1), the Cloudrider has a semi conventional, three lifting surface design. As pointed out in [12] this layout has a significant wetted area reduction potential (about 34% for a business size aircraft).The wide-body fuselage design allows a twin-aisle layout, while further reducing the wetted area pro passenger [13] and the boarding time. To maximize the aerodynamic efficiency, high aspect ratio wings are deployed, equipped with hybrid laminar flow control (HLFC) devices. The special designed rear part reduces the tail interference drag and improves the ruddervator efficiency.

Calculated by the detailed drag estimation of Raymer [14], the presented layout allows a lift to drag ratio (L/D) of 24 in cruise, while the most commercial concepts nowadays provide an L/D around 20.
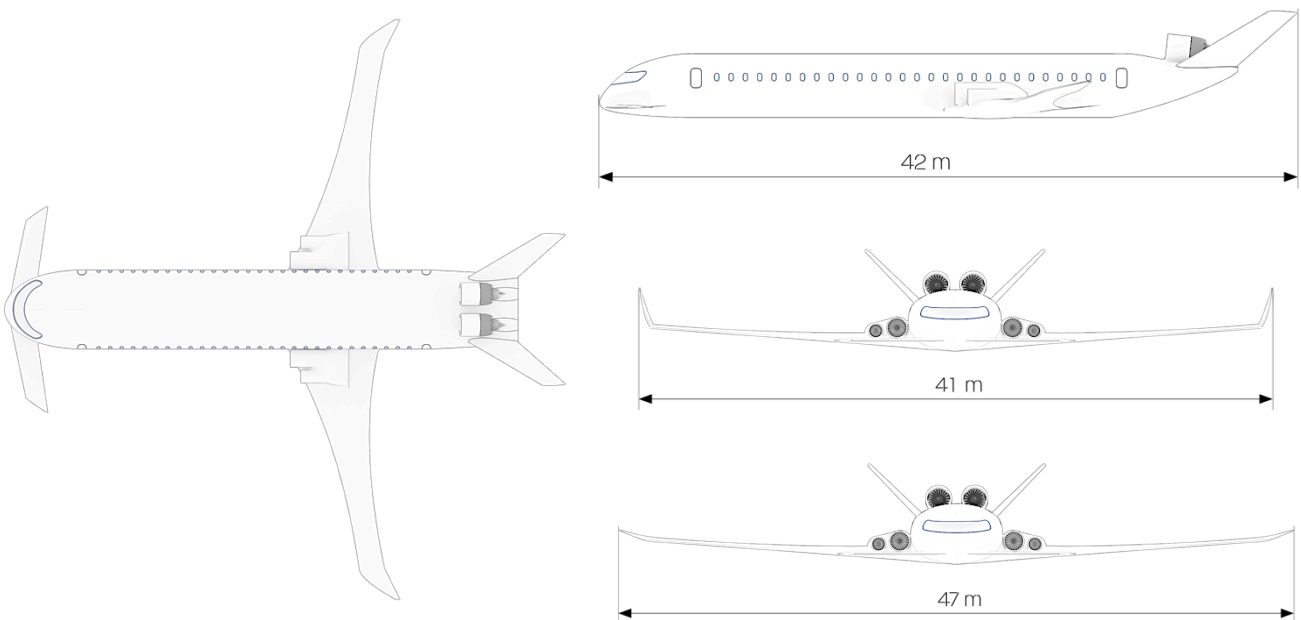
Figure 1.: Main dimensions of the Cloudrider

3.2 Propulsion

The Cloudrider incorporates a hybrid Distributed Propulsion (DP) system which consists of two turbo fans (TF) and four electro fans (EF) with high-temperature-superconducting (HTS) motors. From aerodynamic considerations, the EFs in the wing root are larger than the EFs on the outside. The TF engine uses two energy sources Liquid Natural Gas (LNG) and kerosene, called a Multi-Fuel Hybrid Engine (MFHE), which is coupled with the hybrid-electric DP system. This arrangement we have named Double-Hybrid Propulsion System (DHPS). Due to the constant gas turbine mode of the MFHE, the strategy of the batteries, that there are used only in the take-off and climb segment to provide the energy for the EFs and they will be charged from the MFHE during the cruise segment. This lead to a smaller battery size, enable a to get a larger ETOPS certification and reduce the turn-around time. The electrical system and the MFHE are connected in two different ways. On the one hand, the electrical system is partly powered by the engine in cruise segment. On the other hand, the LNG must be stored on the aircraft as cryogenic liquids which can also be used as a cryogenic cooling system for the high temperature superconducting motors, inverters and other devices. The presented DHPS combined with the novel airframe design enables 60.6%

reduction in energy reduction in payload km compared to the Boeing B737-900ER baseline aircraft. The general arrangement of the Cloudrider is represented on the Figure 2.

HBPR Multi-Fuel-Hybrid Engine

Active wings help to reduce the wing load

Aerodynamic housed HTS electro fans maintaining upper surface blowing

Bell-loaded canard

LNG stored in the fuselage
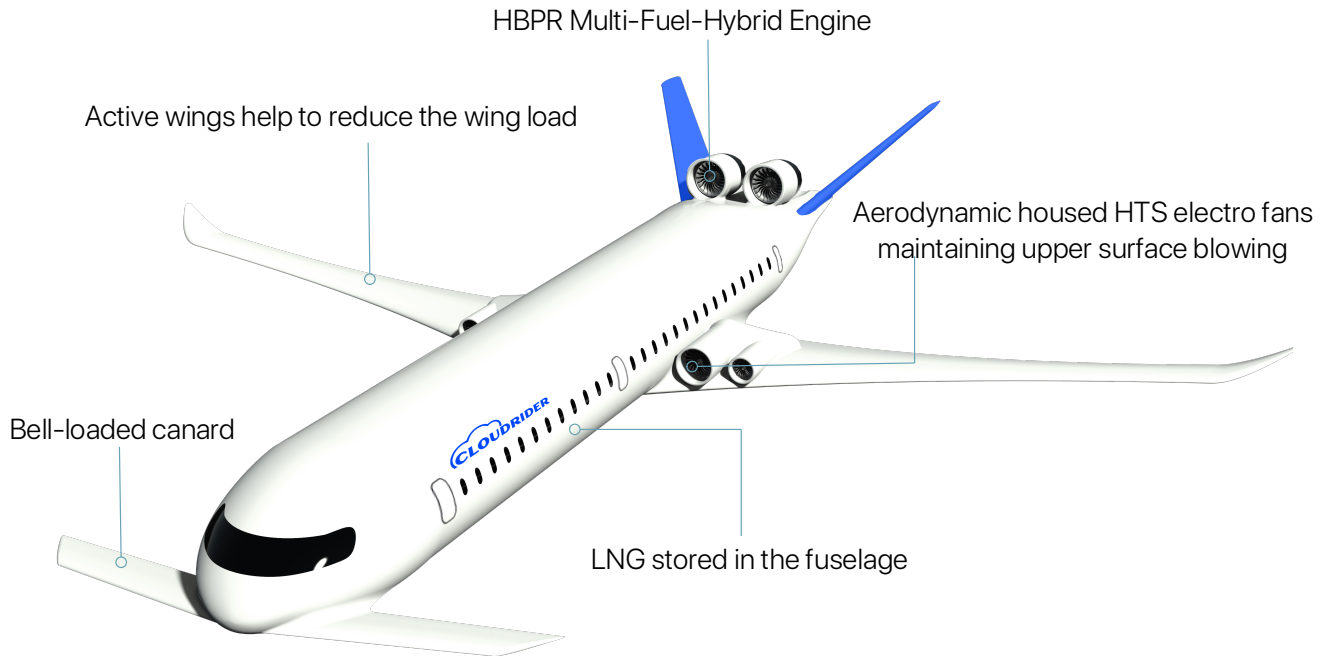
Figure 2.: General arrangement of the Cloudrider

4 Ultra Efficient Aerodynamics

As mentioned above the Cloudrider has to meet the high level – at least 60% total energy saving – standards by 2045. The required energy for a specific mission is generally driven by two main construction factors, mass and drag. The propulsion system has to counteract the losses due to aerodynamic forces and has to provide the required kinetic and potential energy which is needed to accelerate and reach the required altitude. Therefore, it is clear, that for reaching the standards written in the Introduction, drag reduction is essential.

4.1 Drag reduction in general

The two main sources of aerodynamic drag for an average commercial transport aircraft in cruise are the skin friction and the lift-induced drag, up to ca. 50, and 30-40 percent of the total drag [15]. As skin friction drag has generally greater role at higher airspeeds, it has a great energy saving potential for cruise, which takes up the majority of the mission time. Nevertheless, the induced drag cannot be neglected as well, especially in take-off.

If one does not consider the laminar or turbulent nature of the flow, the friction drag depends primarily on the total wetted area of the aircraft. The lift induced drag depends however more on the aerodynamic layout, and the wing load distribution. The Cloudrider concept attempts to minimize the wetted area, while deploying high efficient aerodynamic solutions, thus reaching an improved lift to drag ratio.

4.2 Perspectives in general arrangement

At the start of the design process the basic question was, if we should orientate towards the conventional tube and wing (TAW) layout or create a completely new and unusual concept. In the past century, several basic aerodynamic layouts were analyzed and some of them also built. This section gives a short review about the possible conceptions and their properties.

A radical, promising one is the blended wing body (BWB) layout, which could theoretically result a better lift to drag ratio then conventional configurations since almost the whole aircraft produces lift. However, various research and analysis showed [16], that an efficient BWB realization has a minimum seat capacity of ca. 600 passengers, not to mention the cost of various completely new technologies, new standards, safety issues [16] and the public acceptance.

For the defined seat capacity, the twin-fuselage aircraft concept could be another viable alternative [16]. It has some good potential as well, thanks to the lower loads, therefore lighter structural weight. Considering the facts that the usually very large wingspan requires much wider airport boxes, and the two fuselages need a special boarding system, an economical market entry in 2045 seems to be unrealistic, because it would require major infrastructure changes at the airports.

As it was pointed out in [17], a PrandtlPlane (PrP) box wing configuration would be a viable alternative as well, because it provides a theoretical minimum for induced drag. However, the size of the total wing surface increases the viscous drag significantly. Even with NLF it would require additional systems, due to the large chord length.

According to [18] (under the specified size and mission requirement the aerodynamically optimum is somewhere between the conventional TAW layout, and the BWB construction. However, required structure mass, the reaction of the market and development costs still have to be kept in mind.

Further literature analysis showed (Torenbeek [16], Gudmundsson [19], Raymer [14]) that a semi-conventional three surface canard design with lifting body and high aspect ratio wings seems to be a promising choice.

4.3 Greener by design

The introduction of advanced basic technologies, such as the major improvement in the field of composite materials and the increasing safety levels of digital and electronic solutions open new perspectives in the aircraft design as well.

4.3.1 Laminar flow control

According to [15] laminar flow control can maintain up to 15% drag saving. The laminar-turbulent shift can be delayed by using active or passive techniques.

As Selig [20] states, below $RN = 20 \cdot 10^6$ natural laminar flow (NLF) airfoils are decent. The RN in cruise ($9 \cdot 10^6$) at the outside region of the wing is still below this limit, so NLF are feasible here. However, in the inside of the wing the Reynolds Number is almost 5 times higher, and a NLF profile alone would not be enough to control the laminar-turbulent transition. Therefore here, and on the tail as well, boundary layer suction is applied.

For the preliminary design phase the NLF0115 airfoil was chosen. This has a well-documented [20] behaviour, and suits well the Cloudrider's cruise condition requirements (C_L=.0.61). Nevertheless, in the further design a specially engineered airfoil has a further drag saving potential, as can be seen for example in the NASA's NLF airfoil development [21] report.

With an active skin technique, described in [15], an additional transition delay and up to 2% drag reduction on the fuselage can be achieved.

4.3.2 Wing Design

The main goal of the Cloudrider's wing design is induced drag reduction, which is inversely proportional to the aspect ratio. While keeping AR as large as possible, calculated with the equation of Korn

[22] for the chosen airfoil a slight wing sweep of 13° is still required to stay below the critical Mach number in cruise. Thus, a wing sweep of 15°was chosen to minimize the induced drag while still avoid the wave drag and maintain some freedom for an occurrent airfoil change. The low sweep keeps the attachment line instability at low level as well, which is generally favorable for NLF profiles.

According to Reist [18], the optimal aerodynamic shape of an airplane is somewhere between the BWB and the conventional TAW configurations, primarily depending on the aircrafts size. Thus, after numeric optimalisation, the Cloudrider's taper ratio is kept small (0,2), and the wing root chord large (10 m), to approximate the optimum, and reach the maximal L/D ratio at the design point in cruise conditions.

The wingspan is 48m, with a 3.5 m folded up wingtips on both side. This solution is already certificated and applied by Boeing on the 777s. Although it makes the Cloudrider 2 m larger then the current largest box standards (39 m), but recent trends show an increasing average wingspan [5], thus in 2045 generally larger airport boxes can be expected. Until that the parking is maintained in the 36 and 39 m boxes with parking assistance.

The wings are equipped with raked wingtips, which can maximize the drag saving up to 15 percent [23]. The smooth, blended transition however helps to further reduce the interference drag.

4.3.3 Canard with Prandtl-load

Another key feature of the Cloudrider concept is the bell-loaded canard wing on the front of the plane.

Since 1903 – the first flight of the Wright brothers – canard construction has been a well-known aircraft concept. In theory (reference), it can maintain a pitch control with less induced drag, since the required nose up momentum is not provided by the downward pointing forces of aft-placed horizontal stabilizers, rather by the lift of front placed stabilizer wings, the so-called canards. If carefully designed the safety from stall can be another positive property. On the other hand the designer should consider the additional problems caused by this construction, e.g.: the disturbance in the flow field after the canard, and its negative effect on the wing, longer take-off and landing slopes or the induced drag of the canard. Considering these reasonsr, one can see clearly that a good canard design is hard to maintain, but it has some promising benefits as well.

A well-known fact is, if the wing of the aircraft has to satisfy some fixed geometric conditions, then for a given lift coefficient the minimum induced drag is achieved by the application of an elliptic span load. However, Prandtl published an article in 1933 [24], in which he derived the minimal induced drag with a different approach. I.e. the total lift is the same, but instead of the span, the bending moment is fixed (this condition is more or less equivalent to a fixed structural mass). The solution provided a new, so called bell-shaped span load. For the same lift coefficient, it provides a 11% less induced drag, with a 22% wider span and (almost) the same structural mass. An additional feature is a different downwash field, especially at the wingtips (from 88% span), where the wing has an up wash. This results in a perverse yaw characteristic, as it was proven by NASA in the [25]. It is interesting to mention that -independent from Prandtl- the Horten brothers applied this kind of span load as well, to control their all-wing aircrafts.

Combining the above features, canards and bell-shaped loading, some beneficial results can be achieved. The smaller induced drag extends the aerodynamic efficiency, and the disturbing effect of the softer canard down flow field (smaller vorticity) on the main wing is reduced as well, as it is pointed out in [26] also. The large horizontal difference between the main wing and canard further cuts down on the disturbing effect, this was proven with the method published in [27].

The upwash characteristic of the canard tips indeed perfectly suits the Cloudrider. With the elliptic span load of the main wing would normally be in the downwash field of the canard. Basically, this should not cause a real problem even with elliptic load, because for the configuration the elliptic canard would be not wider than the inner part of the main wing, partially housing the electric turbofans. Although the bell-loaded canard is 22% wider, it's upwash at the wingtips avoids the clean flow regions of the main wing, even if the inner part is in downwash. At a fixed vertical canard and wing placements these phenomena occur, of course, at different angles of attack for elliptic and bell load.

The canard design is based on Strohmeyers detailed three lifting surface aircraft calculations [28], the most effective canard layout can be realized with a low position, swept back canard. Thus the canard has a 2 m wingroot, with a 11 m wingspan.

The canard is placed to the front, to maximize the lever arm and thus the reachable pitching moment.

On the whole, the above written features make it possible to eliminate the biggest disadvantages of the canard configuration, provide more aerodynamic efficiency, thus more economical flight, and positive changes in the control characteristic as well. However further aerodynamic CFD, and wind tunnel experiments are required to determine the exact effect.

4.3.4 Vee-Tail, stability and trim

Regarding the possible conventional vertical and horizontal stabilizer configurations from an aerodynamically point, the V-tail is the most effective one [29]. V-tail has less interference drag and improves directional stability at high sideslip angles. It has to be mentioned here, that the ruddervators require a complex control system, because t, but it is already conventionally maintained on other V-tail models, and because of the recent fly by wire standards this is expected to be solved at 2045.

Although – through fly by wire stabilized – naturally unstable airplanes have some really promising possibilities for example with wetted area reduction, the Cloudrider is designed to be naturally stable, with a lateral stability factor of. If a worst case scenario occurs, a defensive design strategy can save many lifes.

The change of the center of gravity is 1,78 m, with a maximum -54% stability in the landing phase. The worst value is -28% without payload in take off.

The canard is equipped with flaps, and the ruddevators allow an additional precise pitch control. Owing to the large distance between CG and the canard, the three surface layout allows the reduction of the trim drag, while providing stability and good handling properties as well. A detailed explanation can be found for example in the Piaggio 180's documentation [12]. The occasionally lift reduction on the main wing caused by the canard is minimized as well (explained in 4.3.3).

In addition to the conventional devices, the Cloudriders fast actuated electrofans are capable for helping out in yaw control. However, their effect is limited, due to their near fuselage position.

4.3.5 High lift systems

The high lift required in takeoff is ensured by nonconventional, actuated wing flaps. The morphing flap feature has several favorable properties [30], it generates lower noise and drag, while providing the same lift enhancement. According [30] a 84% improvement in the L/D can be reached.

The electric fans in the wing roots maintain a significant additional lift coefficient in take–off, with additional flap blowing system a maximal local lift coefficient of 6 can be reached. [31], this means a 0.4 lift increment for the whole wing.

The pusher arrangement of the engines helps to gain additional lift on the ruddervators as well, because they are located between the tails.

4.3.6 Mass reduction

Generally, researchers predict that advanced composite technologies will allow an approximately 10% [16] mass reduction in aviation in the next decades. The structure mass estimation of the Cloudrider concept was based on conventional methods (Roskam, [32]) , and after that the predicted mass saving was calculated as well. It was assumed, that in 2045 a general 10% reduction in structure mass will be achievable.

Components	[kg]
Fuselage	12300
Landing Gear	2300
Control Surface	2300
Wing	9500
Propulsion	
System	5800
Systems	28000
OWE	61400
Payload	31500
LNG	12700
Kerosene	4700
Battery	3900
MTOW	114200

Figure 3.: Main components weight table

However, the conception allows further mass save:
- The propulsion system, and wing arrangement allow shorter landing gears
- For maneuvers a wing loading alleviation system is installed, this allows a further reduction of the total wing mass.

5 Double-Hybrid Propulsion System

The focus of the Cloudrider concept is to achieve dramatic energy efficiency improvements in accordance with the NASA N+3 upper far-term target of 60-80% reduction in energy consumption. Examining radical ways in abating the anthropogenic impact aircraft operations have to the environment, we decided to undertake a comprehensive inter-disciplinary design and integration project where hybrid propulsion systems would be the basis for providing motive power to the aircraft. This concept includes a novel hybrid DP system which consists of a TF engine uses two energy sources: LNG and kerosene. This is called Multi-Fuel Hybrid Engine (MFHE), which is coupled with the hybrid–electric DP system. This arrangement we have named Double-Hybrid Propulsion System (DHPS) as above has been mentioned. The presented sizing and optimizing methodology of hybrid-energy aircraft system with the novel airframe design enables 60.6% reduction in energy in payload km compared to the Boeing B737-900ER baseline aircraft. The resulting electric system is combined with the unconventional MFHE technology which is down-selected from a number of multivariable MFHE cycle optimization studies that were conducted in the flexible modeling environment CycleTempo®. The resulting engine performance is compared to current Open Rotor (OR) and TF technologies and potential improvements in fuel consumption and NO_x emissions are presented.

5.1 Distributed Electric Propulsion System (DEP)

Encouraged by the progress made in the automotive industry, aeronautics found an interest in hybrid propulsion and this process will provide an advancement in the future battery technology. An idea is to merge this concept and distributed propulsion, where the engines are distributed along the wing. The increased performance of the Distributed Electric Propulsion (DEP) in fuel consumption, noise, emission and handling qualities was shown in previous studies [33, 34]. The results demonstrated a drag reduction (which leads to lower fuel consumption) and also a better efficiency due to the aero propulsive effects. The

four superconducting Electro Fans (EF) in the Cloudrider are located in the upper part of the wing, at the trailing edge. This allows some advantages in terms of blowing, which has been investigated in the international CleanSky project of the EU [7, 35]. An additional efficiency gain of the DP appears possible if this boundary layer is "ingested" and accelerated by the fans, because it can reduce the aircraft's wake and hence its drag [36, 37]. Another advantage of the DEP architecture is the EF weight is reduced. In fact, the One Engine Inoperative (OEI) condition (which is assumed as a critical case for the design) is less stringent, as shown by Steiner et al. [38].

5.2 Investigation of Alternative Fuels

The increase of aviation traffic had consequences in terms of greenhouse gases and local pollutant emissions (e.g. CO, HC, NO_x). In order to minimize this problem, the investigation of sustainable alternatives to current jet fuel and its impact on emissions is required. For this purpose, batteries, hydrogen fuels, fuel cells, biomass and LNG were examined as alternative fuels in aircraft application. Most of the fuels investigated and tested were derived from biomass or other forms of organic supply and waste.

Biomass fuels are interchangeable with jet fuels, but typically do not offer any technical advantages unless modified to withstand higher temperatures [39]. Most of the common barriers were related to environmental, technological, economic and social issues etc. competition with edible biomass (food, feed) and low energy density [40].

A key criterion for batteries in aircraft application is the specific energy density. Li-Ion batteries, today, are limited to energy density below 300Wh/kg which is approximately 2.5% of jet fuel [8, 41]. There are different predictions for the future energy densities mostly in the range of 750 to 3500 Wh/k [42, 43] in a 2035 timeframe. To achieve this improving in energy densities receives a great amount of research and technological advancements in battery materials are expected to enable higher densities [41]. Based on these estimations the Cloudrider concept operate with a more realistic sulfur based battery system with on energy density of 1500 Wh/kg for the EIS 2045 timeframe [41].

Another fuel option could be the establishment of cryogenic fuels such as LNG and liquid hydrogen (LH_2). Both of these fuels have a higher mass specific energy (*LNG ~ 50MJ/kg; LH₂ ~120 MJ/kg*) than jet fuel but a lower volumetric density (*LNG ~22MJ/kg; LH₂ ~8MJ/kg*). This results a reduction in aircraft operating weight and a loss of cargo space to cryogenic fuel storage [44]. Hydrogen is a highly reactive gas, and as such it tends to react with the metals commonly used in engine design [45]. Additionally, the production of *LH₂* suffers from severe drawbacks as long as the methods rely on steam reforming of natural gas which lead to a high energy and greenhouse gas footprint compared to conventional jet fuel [46]. In contrast, LNG is one of the cleanest fuel, and recently it has been shown that LNG can also be generated by using renewable energy [47, 48]. Moreover, the reduction in total LTO *NOₓ* is estimated to be 85% compared to the B737-900ER baseline, which is shown in the results of the engine optimization in section 5.4 [49]. NAA has studied fundamental technical aspects of using LNG in for-purpose designed aircraft, and no technical barriers were found that would prevent the use of natural gas as an alternative aviation fuel [50]. Because liquid hydrogen is expensive to produce, it is not an economically viable option compared to LNG or conventional jet fuel at current market conditions. Nevertheless, LNG cannot be stored in wings and need an insulated cylindrical or spherical tank in the fuselage. This is a trade-off between the storage strategy of the fuels. However, due to the light wing structure of the Cloudrider, it cannot hold a large amount of fuel.

The Cloudrider concept incorporate a multi-fuel system which consists of jet A fuel, batteries and LNG for the power generation. This was done to fulfill the strict energy and emission reduction requirements and as a result of a complex trade-study of the above-mentioned properties of alterative aircraft fuels. The multi-fuel system makes the optimization process more complicated (see in section 5.3.5), but also required a novel handling process in the ground operations, which is discussed in section 6.1 in more detail.

5.3 Double-Hybrid Propulsion System Architecture

To achieve more than 60% fuel burn reduction and 80% reduction of LTO *NOx* emission [51] the continuous improvements of conventional technologies may not be sufficient to fulfill the aggressive requirements. One potential method is the investigation of forward-looking integrated energy–power system configurations. The NASA project SUGAR [45] executed by Boeing has shown that the integration of a hybrid battery and conventional engine propulsion system enables dramatic reduction in mission fuel burn for long-medium-range application. The Cloudrider concept therefore introduces a novel hybrid technology, which integrates a combustion system powered by LNG and kerosene with the electrical energy linked to the characteristics of superconducting electric motors technology.

Various distinct hybrid electric propulsion system architectures are possible [52]. A detailed representation of the Cloudriders propulsion system is introduced in the Appendix. A Series/Parallel Partial Hybrid [39] configuration was selected. In this system, the aircraft uses the combination of a combustion engine (CE) system powered by fuel and an electrical system using the electric energy of batteries and the engine coupled with the generator. In the Cloudrider concept the combustion engine is the MFHE powered by LNG and kerosene fuels, which in section 5.3.5 will be discussed in more detail. That two systems are connected in two different physically ways. On the one hand, the electrical system is partly powered by the engine in cruise segment. On the other hand, the LNG must be stored on the aircraft as cryogenic liquids which can also be used as a cryogenic cooling system for the high temperature superconducting motors, inverters and other devices. The cryogenic cooling system is be explained in section 5.3.1**.**

5.3.1 High Temperature Superconducting Devices & Cryogenic Cooling System

One of the most important component of the DHPS system in the Cloudrider concept is the application of HTS technologies to reduce electrical power transmission losses and weight penalties [53]. Current-day superconducting machines (with resistive armature) are comparable with turbine engines in power density, while fully superconducting machines have the potential to be 3 times lighter [54]. In the Cloudrider concept both generators and motors are assumed to be fully superconducting, considered the EIS 2045.

A disadvantage of HTS devices is currently the cooling system, which requires cryogenic cooling to keep the HTS material at required temperature. Since there will be electrical benefits for the superconducting components using the lowest possible temperature, the trade between efficient and light cryogenic cooling and the low temperatures that minimize AC losses and material usage will be important [55]. In the Cloudrider concept the cryogenic LNG tank provides the heat for the fully centralized Cryogenic Cooling System (CCS) for the HTS motors, inverters and other superconducting devices. Yttrium barium copper oxide (YBCO) family of superconductors includes the first material that was discovered to become superconducting above the boiling point of liquid nitrogen (77 K) at about 93 K [56]. Previously the record was held by the cuprate materials, which have demonstrated superconductivity at atmospheric pressure at temperatures as high as 138 K, and 164 K under high pressure [56]. It can be seen, that there are no physical barriers to achieve a higher Superconducting Temperature (ST) in a 2045 timeframe. The CCS must provide the superconducting temperatures for the materials and balance the heat generation of the system. The heat generation of one 1 MW HTS motor using the YBCO materials are the following:

- 1.8 Watt heat generation from the resistive connections and equivalent resistance of the coils [57].
- Heat transfer rate of the HTS motor with an overall heat transfer coefficient U, ΔT temperature difference and A cross section area was calculating from the equation:

$$q = U \, A \, \Delta T$$
<div align="right">Eq. 1.</div>

The conduction coefficient k can be found from the resistance network where:

$$R_{total} = \frac{1}{U\,A}$$

<div align="right">Eq. 2.</div>

- 5 Watt heat load from the radiation effects of the cryostat [57].

These results were accomplished with 63 Watts of cooling from the CCS for one HTS motor. The refrigeration power of CCS can be found from the equation:

$$Q = c\,\dot{m}\,\Delta T$$

<div align="right">Eq. 3.</div>

ΔT is the temperature difference between the refrigerant and the required ST, c is the heat capacity and $\dot{m}$ is the flow rate of the refrigerant. There is no significant difference between a motor and a generator and the HTS motors were treated in exactly the same fashion as the generators. Furthermore, it was assumed that they are driven by cryogenically cooled inverters so that the shaft speed of the fans can be varied independently of the generators. From the thermal calculations of the HTS devices, considered the EIS 2035, we get a refrigeration power of 463 Watts with the cold head kept at constant 138 K. The freezing point of the LNG is 90 K, which provides enough temperature difference to realize CCS using the heat of the LNG with the given entry into service horizon.

5.3.2 Top Level Aircraft Requirements & Mission Profile Optimization

The Cloudrider concept shall conform to the future market-driven top-level requirements for the medium to large range market, taking into account that an aircraft with an EIS 2045 will need to operate within the boundaries of existing infrastructure and standard operational procedures of conventional aircraft. The mission profile of the Cloudrider concept fulfilling the EU OPS 1.225 [58], which consists a climb to TOC point within 25 min, at ISA+10°C with the climb speed schedule 250 knots (130 m/s) / 270 knots (140 m/s) / M0.75 (220 m/s). Followed by a constant altitude cruise at FL320, M0.75, ISA+10°C and ended by a climb-mirrored speed scheduled for descent. Cruise, descent, loiter and approach do not affect the battery sizing due to the battery charging in cruise, which will be discussed in section 5.3.3 in more detail.

Cruise altitude must be greater than FL310 in order to permit operational flexibility and have ability to fly over weather [8]. To identify the cost optimized flight profile the Energy Specific Air Range (EASAR) [8] is not valid anymore for multiple energy sources, which have different market prices. Therefore, a figure-of-merit (FoM) considering the energy cost is more appropriate for flight technique optimization of hybrid-energy aircraft. The COst Specific Air Range (COSAR) with unit [m/USD] was introduced by Pornet et al [10]. In the case of Cloudrider the COSAR can be written as:

$$OSAR = \frac{V \cdot L/D}{(TSPC_{Ker+LNG+Elec} \cdot (y \cdot c_{Ker} + (1-y) \cdot c_{LNG})) \cdot W}$$

<div align="right">Eq. 4.</div>

with

$$y = \frac{\dot{m}_{Ker}}{\dot{m}_{Ker} + \dot{m}_{LNG}}$$

<div align="right">Eq. 5.</div>

where, V is the flight speed in [m/s], W represents the gross-weight of the aircraft [N], L/D is the aerodynamic efficiency, c is the specific cost of fuels with unit [USD/kWh], $\dot{m}$ is the mass flow rate of the fuels [kg/s] and $TSPC$ is the Thrust Specific Power Consumption [W/N]. In the Cloudrider concept is not needed to calculate with the price of electricity, due to the fact, that the butteries are charging from the gas turbine during the cruise segment. TSPC was introduced for hybrid energy aircrafts, because the Thrust Specific Fuel Consumption (TSFC) [40] is invalid for different types of energy.

$$TSPC_{Ker+LNG+Elec} = \frac{P_{Ker+LNG} + P_{Elec}}{T}$$

<div align="right">Eq. 6.</div>

where, P the power extracted from the different energy sources [W] and T is the Thrust [N]. With the TSPC values taken from the CycleTempo® simulation at a specified design cruise speed of M0.75, the COSAR values were calculated for different altitudes (FL310-350). COSAR has the highest value in cruise at FL330 (ESAR=$3.77 \cdot 10^{-4}$ m/$ at M0.75). Consequently, the optimal flight technique is M0.75 at FL330.
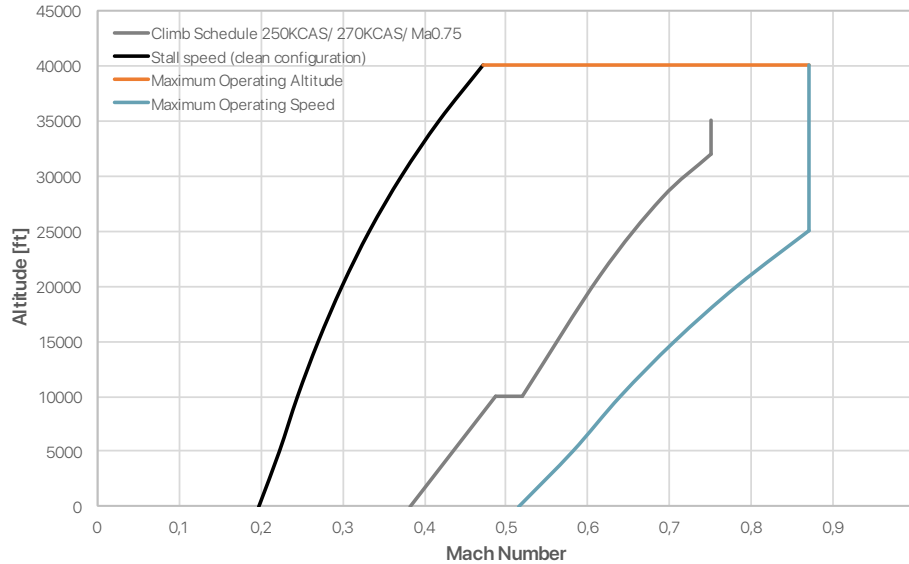

Figure 4.: Flight envelope of the Cloudrider

The flight envelope for the Cloudrider concept is presented in Figure 4 The outer edges of the diagram, the envelope, show the possible conditions that the Cloudrider can reach in straight and level flight. The diagram contains the Stall speed at clean configuration, the Maximum Operating Altitude/Speed and a Climb Schedule as well.

One of the most relevant point for the propulsion system design is the compliance with the airworthiness regulations CS-25 and FAR25 [59] transport category is required and to ensure a safe take-off even in the unlikely event of an engine failure. The main criteria are analyzed for low-speed performances the takeoff-, landing-field length and the climb gradients [60]. For high-speed performance, the residual rate of climb (ROC) during the top of climb (in the case of Cloudrider 300 ft/min) and at en route condition (usually 100 ft/min), considered the safety factor of 1.2 [53] and the OEI drift-down as well. To fulfill the FAA and ICAO regulations the ROC must be at least 100 ft/m in the case of OEI [61]. The rate of climb (ROC) of the segments were kept at the same value as in the case of the Boeing B737-900ER baseline aircraft. According to Extended Range Operations (EROPS) the aircraft has to store enough energy at least for 90 minute single-engine flight to the nearest suitable airport to get the ETOPS 90 certification.

5.3.3 Sizing scheme for the double-hybrid propulsion and performance

The methodology developed for sizing and performance assessment of the double-hybrid Cloudrider will be presented in this section. Second, the integrated performance analysis will be used to compute the required thrust at mission segments. Finally, the MFHE will be optimized in the flexible modeling environment CycleTempo®.

The propulsion system based on constant gas turbine operating mode, which means that the power of the gas turbine is predefined and the MFHE runs at its most efficient point during the majority of the mission. The EFs are sized to the difference between thrust required at take-off and the thrust provided to the gas turbine at its optimum point. The major strategy of the batteries, that there are used only in the take-off and climb segment to provide the energy for the EFs (HTS motors). The batteries will be charged

during the cruise segment use the remaining power of the MFHE (as electrical power off-take). This strategy of the batteries brings three major advantages: the required battery size for an ETOPS certification
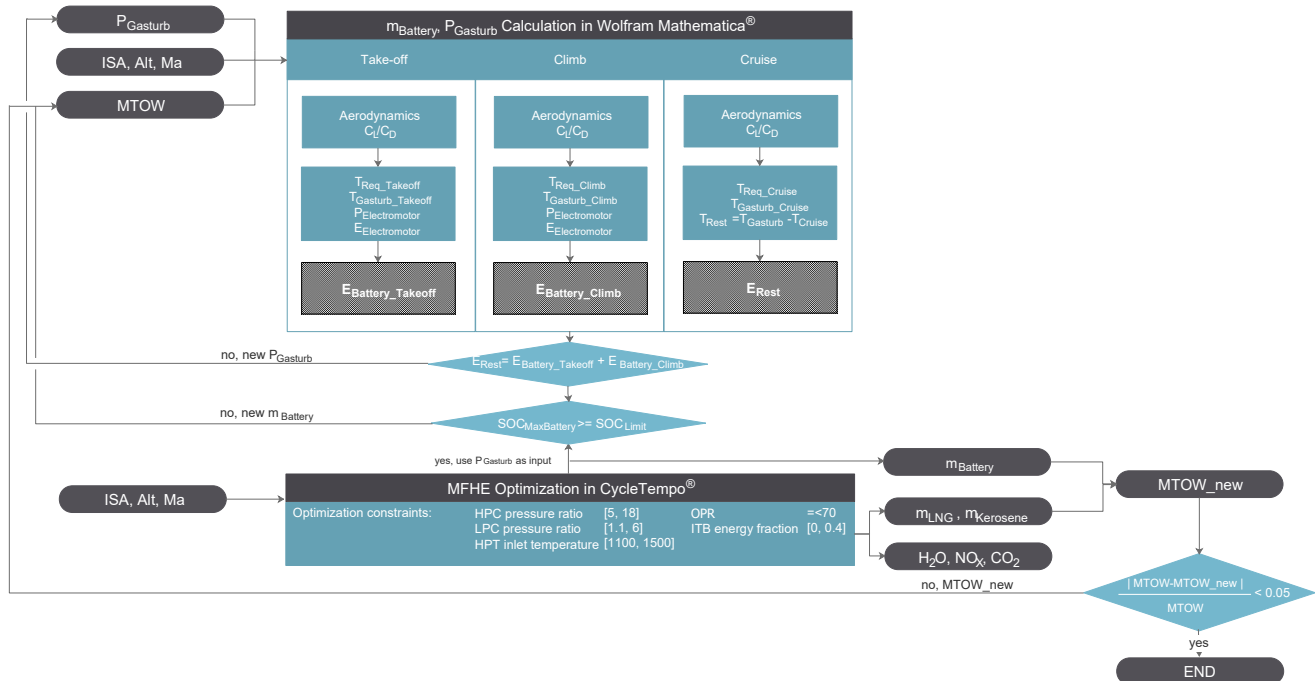
could reduce, decrease the turn-around-time and it is not necessary to change the butteries during the ground handling process.

Figure 5.: The sizing process of the DHPS

As a means of delivering a comprehensive representation of the methodology, the flow process for the sizing of hybrid-energy aircraft is presented in Figure 5. The optimization of the resulting double-hybrid system was divided in two parts. The first part of the process was performed based on in-house developed model implemented in Wolfram Mathematica® [62] to estimate the required battery mass for a given set of Top Level Aircraft Requirements (TLAR). In this process is required, that the remaining energy of the MFHE in the cruise segment must be equal to the energy of the batteries, which provide that the batteries will be fully charged at the end of the cruise phase. One more criteria is, to protect the battery from irremediable damage, if the state of charge SOC is below a certain limit, then the installed battery mass has to be increased iteratively [60]. Consequently, if both criteria are fulfilled than the battery mass is computed and the specified shaft power can be applied as an input parameter for the cycle simulation.

In the second part of the sizing process, to achieve the required fuel consumption and NO_x reduction, the MFHE cycle was simulated and optimized in CycleTempo® [63]. For that simulation, the output parameter of the implemented code ($P_{Gasturb}$) is input parameter for the thermal cycle model, so in that way is the numerical simulation and the analytical method connected. Therefore, this two methods together give us the optimal shaft power of the gas turbine and the MTOW for the design range 7000 km (3780 nm). The complication in this optimization process is due to the fact that the implemented model in CycleTempo® is optimized at a given shaft power, in order to minimize fuel consumption. However, the optimal shaft power is a result of the implemented code, which uses the fuel mass (in MTOW) as an input parameter. This optimization process is then based on an iteration between the thermal simulation and the analytical battery sizing method. Table 1 summarizes the parameters of the involved components in the propulsion system

LFL (Wet Runway) @ ISA, SL	m	1904	1730	1500	-21,2%	-13,3%
MTOW / PAX / Range	kg/PAX/km	0,067	0,073	0,054	-18,8%	-25,6%
Energy Consumption	kJ/100 PAX/km	80008	158304	32401	-59,5%	-79,5%
Energy Consumption	kJ/payload/km	7,48	7,88	2,95	-60,6%	-62,6%

Table 1.: Mass of the propulsion system

Component	Mass sizing parameter	Unit	Efficiency [%]	Source	Total mass [kg]
HTS Motor	21,3	kW/kg	99,7	Vratny et al.	338,0
Converter/ Controller	20	kW/kg	99,5	Brown et al.	135,8
SSPC	44	kW/kg	99,5	Brown et al.	61,7
Transmission	9,2	kW/kg	100	Brown et al.	295,3
Battery	1500	Wh/kg	90	Bogaert et al.	3898,7
LNG	50	MJ/kg		Feijia et al.	12771,6
Kerosene	42,8	MJ/kg			4723,8
Gas turbines				Hove	4790,0
Crycooler					53,2
Summa					27068,1

5.3.4 Energy and Thrust Table

A full description of the DHPS requires three descriptors involving account of the three alternative energy sources and that of the entire propulsion system: one ratio is the power split (H_P), which comparing each of the maximum installed powers; and a second ratio comparing the extent of energy storage (H_E), which was introduced by Pornet et al. [53]. For the sake of completeness, it must be introduced an additionally ratio, the Inter-stage Turbine Burner (ITB) energy fraction, which comparing the mass flow rate of the two liquid energy sources (LNG and kerosene) in the MFHE [64]. These parameters describe the Degree-of-Hybridization (DoH) of the propulsion system of the Cloudrider.

$$H_P = \frac{P_{ELEC}}{P_{TOT}}; \qquad H_E = \frac{E_{ELEC}}{E_{TOT}}; \qquad ITB\ EF = \frac{\dot{m}_{ker} \cdot LHV_{ker}}{\dot{m}_{LNG} \cdot LHV_{LNG} + \dot{m}_{ker} \cdot LHV_{ker}} \qquad \text{Eq. 7.}$$

where, $\dot{m}$ is the mass flow rate of the fuels [kg/s], LHV is the Lower Heating Value of the fuels [MJ/kg]. For a conventional kerosene based gas turbine propulsion system H_P=0, H_E=0 and $ITB\,EF$=1. The values of these descriptors for the Cloudrider concept are presented in the thrust-energy table in Table 2. In this table, the supplied power ratio (ϕ) also presented, which is defined as the total electric motor power
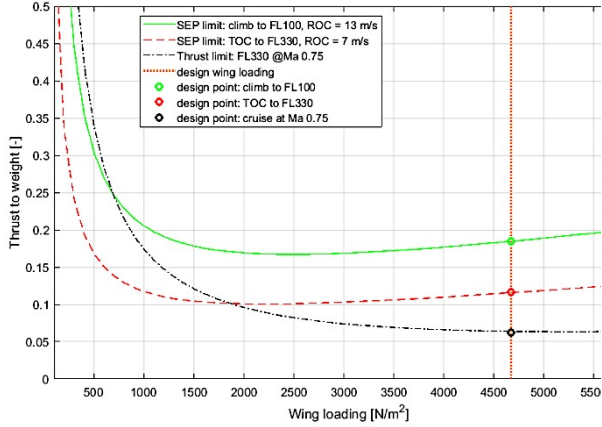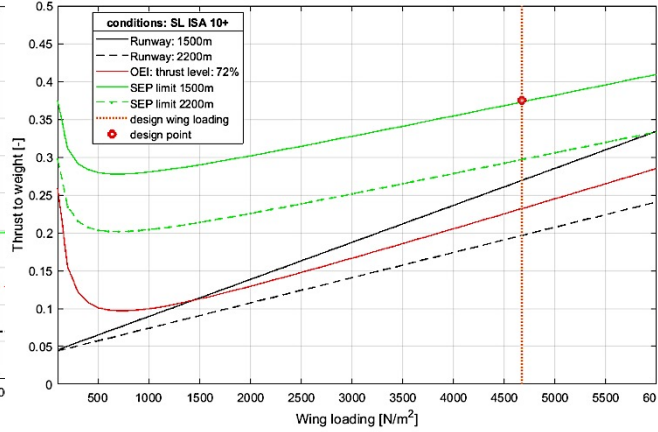

Figure 6.: Constraint Chart for T/O   Figure 7.: Constraint Chart for the Climb

over the mission segments in relation to the total shaft power integrated over the segments.
The required thrust is computed by resolving the flight mechanical equations at each point of the segments according to the flight state (ISA, Alt, Ma), which was done in the performance Constraints Chart (see Figure 6; Figure 7). The EFs than has to compensate the undersized TF performance during the take-off and climb segment as already has been mentioned. In the cruise segment, where the TF has remaining thrust, the batteries are charging and on the other hand the thrust of the EFs were set at 10% of the required thrust in the cruise phase, which is enable that the boundary layer is "ingested" and accelerated by the EFs. In the descent, loiter and approach phase no power is provided to the fans, and the gas power unit will be switched off. The aircraft will be a glider and the energy storage system will provide the power for the aircraft's on-board systems. Hence, these segments are not relevant for the sizing of the battery system and there are not represented in the thrust-energy table (see Table 2).

The double-hybrid DP system with two small TFs instead of a single large TF is considered for the Cloudrider concept. This is a beneficial configuration to get a larger ETOPS certification, which is required for long-haul aircrafts. If the additional energy for a 90 minute flight under OEI will be stored in the batteries it will be lead to a noticeable weight penalty of 10.352 kg, taking into account the weight reduction of the turbofans and mission fuel in the case of single TF. This weight penalty causes a significant reduction in the Energy Specific Air Range (ESAR). ESAR represent the change of aircraft range per change of energy in the system and a convenient evaluation of aircraft performance, because this is independent from the type of energy source [46]:

$$EASAR = \frac{dR}{dE} = \frac{V_C \cdot L/D}{TSPC \cdot m_{A/C} \cdot g}$$

Eq. 8.

where, L/D denotes the lift-to-drag ratio [-], $m_{A/C}$ aircraft mass [kg], V_C is the flight velocity in cruise [m/s] and $TSPC$ is the already introduced Thrust Specific Power Consumption [W/N]. With the assumption that the aerodynamic performance L/D and the cruise velocity V_C is the same, the comparison has been shown, that the single fan method reduces the ESAR by 7.6%.

Table 2.: Thrust-Energy Table

Mission Segments	Taxi-out	Takeoff to 35 ft	Climb to FL100 @ISA+10°C	TOC to FL330 @ISA+10°C	Cruise FL330 @ISA+10°C
Duration [min]	24	0,8	25		530
(DoH) Degree of Hybridization [-]	1,00	0,40	0,52	0,53	0,20
(H$_P$) Power Split [-]	1,00	0,41	0,36	0,38	0,19
(H$_E$) Hybridization factor [-]	0,21	0,21	0,21	0,21	0,21
ITB EF [-]	0,27	0,27	0,27	0,27	0,27
Airspeep [knots]	25	120	250	270	Ma 0,75
Airspeep [m/s]	13	60	130	140	221
ROC [m/s]	-	2	13	7	2,5
Req. Thrust [kN]	24,60	354,25	247,80	110,50	56,43
TFs Thrust [kN]	0,00	220,00	175,50	39,64	50,79
EFs Thrust [kN]	24,60	134,25	72,30	70,86	5,64
TFs Power [MW]	0,00	12,20	12,20	12,20	12,20
HTS EFs Power [MW]	0,24	8,48	7,00	7,38	2,86
TF AUX Power [MW]	0,00	0,55	0,80	0,80	0,85
HTS EF AUX Power [MW]	0,55	0,00	0,00	0,00	0,00
Req. E-Energy [MWh]	0,32	0,11	2,91	3,08	25,24
Req. TFs Energy [MWh]	0,00	0,17	2,71	2,71	115,28
Total Energy [MWh]	0,32	0,28	5,62	5,78	140,51

The TFs of the Cloudrider are positioned on the rear upper section of the aircraft, which is enable the boundary layer ingestion on the fuselage and shield against the fan, jet and turbine noise. A critical point in the positioning of the TFs that they cannot positioned within very close distance which is critical for safe operation [65]. This is in line with the constant power operating mode of the TFs, because they have a small size due to the fact that the MEHE run at its most efficient point during the majority of the mission. In addition, fuel burn-off during en route OEI operations provides an added benefit of accumulating SEP residual with elapsed time, because the aircraft would have the ability of increasing True Airspeed (TAS). This increased TAS is considered important during such emergency modes because the aircraft will have the possibility to reach an emergency or alternate airport in shorter time [66].

Thanks to the battery operating mode and the two small TFs system, the Cloudrider meets the ETOPS 180 requirements, which is a relevant advantage for the long-range operation.

Components	[kg]
Fuselage	12300
Landing Gear	2300
Control Surface	2300
Wing	9500
Propulsion System	5800
Systems	28000
OWE	61400
Payload	31500
LNG	12700
Kerosene	4700
Battery	3900
MTOW	114200

5.3.5 Multi-Fuel-Hybrid-Engine optimization

The MEHE is conceived based on an Inter-stage Turbine Burner (ITB) turbofan engine. This configuration allows the use of different fuels simultaneously. Thanks to that the space usage within an airframe can be optimized with respect to energy storage limited by the increase in fuel volume and the associated aerodynamic drag [67]. Furthermore, the LNG is used in the first combustor, while the kerosene in the ITB. In the optimization process by changing the ITB EF the reduction in engine emissions can be optimized. Previous studies [68] are shown that the use of the very high bypass ratio turbofan can help to improve the engine off-design performance. Due to this the Bypass Ratio (BPR) was set to 15. The reduction in NO$_X$ was achieved with the premixed combustion in the first burner and the flameless combustion in the ITB. Secondly, the engine with sequential combustor has lower maximum operating temperature [69], thereby reduce the NO$_X$ emission.

The configuration of the hybrid engine with two combustors is unconventional: therefore, the customary simulation programs (such as GasTurb12®) are not applicable in that case. Instead, a more flexible modeling environmental is required to model the MFHE concept. In the current optimization process the CycleTempo® is used to model the MFHE. The design point for the simulated cycle was set at Ma 0.75 in ISA condition and shaft power for one engine 6,1 MW (output parameter from the implemented code) at the initial cruise altitude. The take-off and climb conditions were examined with an average value for the altitude and velocity. The cycle optimization is performed to minimize the specific fuel consumption at the majority of the mission (considered with constant gas turbine operating mode).

Figure 8.: The optimized MFHE model in CycleTempo®

The design space and the constraints are defined in Figure 5. The already introduced ITB energy fraction was set to 0.27 as a result of a trade study between the fuel volume and the aerodynamic drag. The plot of the optimization results is represented in Figure 8. In order to compare the engines with TSFC is not possible due to the different energy sources used in MFHE. Therefore, the summation of the energy consumption of the fuels is the basis of the comparison [68]. The optimal value for the HPC pressure ratio is 9.65 and for the LPC pressure ratio is 5. (The power required for the HPC is within the system calculated, hence is not coupled with the shaft of the turbine.) It can be seen from the optimized MFHE cycle that the HPT inlet temperature is 1175.43°C, which is enable the operation without bleed air cooling system (BACS). For the turbine bleeds material were selected a novel ceramic matrix composite (CMC). The use of this material is growing in aviation application because they are 1/3 lighter than the previously used nickel (Ni) super-alloys and can operate at 1316°C temperature, therefore no BACS is needed [70] in the case of constant gas turbine operating mode. The fuel consumption and the NO_X reduction will be discussed in the next section.

5.4 Benchmark Against Reference Aircrafts

In this section will be discussed the main features of the Cloudrider concept with the MFHE in order to indicate the relevant advantages and disadvantages compared to two different baseline aircrafts. In this comprehensive comparison study the reference aircraft needed to reflect technologies at least for EIS 2005. Therefore, the Boeing B737-900ER [71] with EIS 2007 was taken as baseline aircraft. For the sake of completeness, the Cloudrider was compared to the larger Airbus A330-200 [72] as well. Table 3 summarizes the predicted design weights, major performance characteristics and FoM of the baseline aircrafts and compares against the Cloudrider. As can be seen from the table, the MTOW weight is increased by 42,9% (compared to the B737-900ER) due to the additional battery and cryogenic tank

weights for the LNG. On the other hand, the fuel weight (per MTOW) is reduced by 54,7% thanks to the enhanced aerodynamic performance of Cloudrider and the DHPS system. Furthermore, the payload (per MTOW) is higher compared to the A330-200, underlining the usability as freighter after decommissioning from passenger transport, which is in line with the predicted 4.2% growth in air cargo traffic over the next 20 years [2]. One of the most interesting point in the comparison table is the energy consumption of the Cloudrider. The energy was computed from the mass of the fuels multiplied by the Lower Heating Value (LHV) of the fuels (LNG and Kerosene). The parameter for the energy comparison was defined in two different ways. First, the energy per km unit was provided by 100 PAX. In this case the reduction in energy was 79.5% compared to the larger Airbus A330-200, while compared to the B737-900ER the reduction is 59.5%. The second method was the payload specific energy per km unit. With this method, predictions indicate that the Cloudrider represents approximately 60.62% reduction in energy consumption compared to the B737-900ER and 62.6% reduction compared to two A330-200.

For a comprehensive investigation of the Cloudrider concept is required a to compare and contrast the MFHE against at least one appropriately identified reference state-of-art engine. One emerging technology is the contra-rotating open rotor (CROR) [58]. This type of engines offers fuel burn reduction and is seen as a good alternative to turbofan engines for the propulsion of future low to medium range aircrafts [73]. The A319's CFM56-5B6/P [74], the B737-200's CFM56-7B27 [74] and the CROR are the basis of the performance and emission comparison as can be seen in the

A direct TSFC comparison is not possible due to the different energy sources used in the MFHE. Instead, the engine is compared by TSPC as earlier defined in Eq.6. The TSPC benefit of the CROR propulsion compared to A319's CFM56-5B6/P turbofan engine was found to be around 53%.

In contrast against the MFHE the CROR has 7.3% lower TSPC in take-off condition. On the other hand, the open rotor engine comes out slightly heavier primarily due to the heavy and large propellers and rear weight structures [75]. Nonetheless, the noise impact of this technology needs to be acceptable if it is to be adopted commercially. In respect of the noise reduction previous studies have been investigated for the noise shielding [76] and bleed setting methods [77] of the CROR. In addition, the fuel consumption benefits of the open rotor engine increase at lower ranges [78]. However, emerging drone technology may also impact on the open rotor propulsion system in the future.

Table 3.: Performance comparison to the baseline aircrafts

Aircraft Properties	Unit	B737-900ER	A330-200	Cloudrider	Δ (B737-900)	Δ (A330-200)
EIS	Year	2007	1999	2045		
Ferry Range, LRC, ISA+10°C	km	5926	13450	7000	18,1%	-48,0%
PAX	–	215	246	300	39,5%	22,0%
MTOW	kg	85366	242000	114200	33,8%	-52,8%
OWE	kg	44677	120600	61400	37,4%	-49,1%
Payload	kg	23045	49400	31500	36,7%	-36,2%
Payload / MTOW	%	27,0	20,4	27,6	2,2%	35,1%
Cruise Speed	Ma	0,78	0,785	0,75	-3,8%	-4,5%
OWE / MTOW	%	52,3	49,8	53,8	2,7%	7,9%
OWE / PAX	kg/PAX	208	490	205	-1,5%	-58,3%
Fuel Weight	kg	23817	109186	15437	-35,2%	-85,9%
Fuel Weight / MTOW	%	27,9	45,1	13,5	-51,6%	-70,0%
Ref. Area (S_{REF})	m²	124,58	361,6	224	79,8%	-38,1%
Aspect Ratio	–	9,45	9,39	10,3	9,0%	9,7%
Overall Span Length	m²	35,79	60,3	46	28,5%	-23,7%
MTOW / S_ref	kg/m²	685	669	510	-25,6%	-23,8%
TOFL @ ISA, SL	m	2830	2770	2200	-22,3%	-20,6%
LFL (Wet Runway) @ ISA, SL	m	1904	1730	1500	-21,2%	-13,3%
MTOW / PAX / Range	kg/PAX/km	0,067	0,073	0,054	-18,8%	-25,6%
Energy Consumption	kJ/100 PAX/km	80008	158304	32401	-59,5%	-79,5%
Energy Consumption	kJ/payload/km	7,48	7,88	2,95	-60,6%	-62,6%

The novel MFHE design of the Cloudrider combined with the HTS motors and batteries leads to a significant impact on the ecological footprint of the aircraft. To examine the Cloudrider's NO_X emission, the Landing and Take-Off cycle (LTO) cycle conditions were simulated as off-design points for the MFHE performance cycle. A sufficient margin against the ICAO CAEP/6 LTO *NOx* certification limit may be achieved for all the configurations that have been assessed assuming EIS 2045. The reduction in total LTO *NOx* is estimated to be 85% compared to the B737-900ER baseline.

As can be seen from the Table 4 corresponding characteristic value LTO NOX D_P/D_0 would be 84% below the CAEP/6 limit, due to the fact that the engine with sequential combustor has lower maximum operating temperature. The data for the A319's CFM56-5B6/P and B737-200's CFM56-7B27 emissions are taken from the ICAO Emission Database [79]. The data in the table represent only the values for one engine instead of two as in the aircraft configuration.

Table 4.: Engine performance comparison

Conditions	A319 CFM56-5B6/P (2006)	B737-900ER CFM56-7B27 (2007)	CR Open Rotor (2020)	Cloudrider MFHE (2045)	
Overall Length [m]	2,6	2,5	7,1	2,1	
Nacelle Diameter [m]	1,7	1,5	1,7	1,4	
Rotor diameter [m]	N/A	N/A	4,2	N/A	
Engine + Nacelle Weight [kg]	2378	2366	4181,2	1955	
Thrust in Take Off [kN]	104,5	121,4	121,3	104,2	
TSPC in Take Off [W/N]	395,4	455,3	183,9	198,4	
				LNG (Combustor)	Kerosene (ITB)
Fuel Flow in Take Off [kg/s]	0,966	1,292	0,521	0,402	0,176
ICAO Landing and Take Off Cycle [g/kg fuel]					
T/O	39,2	30,9	14	5,8	10,2
Climb Out	28,0	23,7	9	3,5	8,8
Approach	9,9	11	9	0	0
Idle	4,5	4,8	5	0	0
BPR	5,9	5	N/A	15	
OPR	33,1	28,3		<70	
LTO NOx D_p/F_0 [g/kN]	46,9	64,1	12,1	8,4	
% below CAEP/6 limit	8,8%	2,80%	79%	84%	

5.5 Uncertainties Management

In this section is the effect of a more hybrid (electrical) propulsion system investigated. A parallel-hybrid architecture was chosen and the DoH (or supplied power ratio) [53] was varied (so-called constant power split (H_P) operating mode) for multiple energy densities of the battery. For this purpose, the modified Bréguet range equation in the form introduced by von Bogaert et al. [80], with the modification in the fuel energy density due to the LNG and Kerosene energy sources (ITB EF was also defined in the equation).
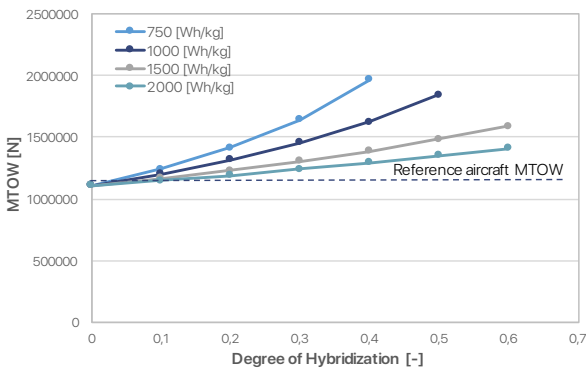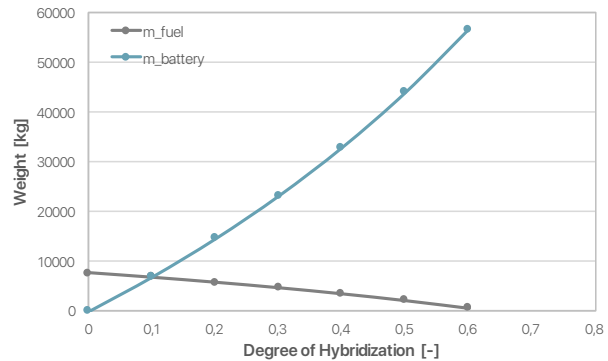

Figure 9.: MTOW in function of DoH

Figure 10.: Fuels weight in function of DoH

The design point was specified in the cruise segment, used constant H_P, which is approximately equal to the supplied power ratio (DoH). On Figure 10 can be seen that for a range of 7000 km, the fuel weight decreases with an increasing DoH. On Figure 9 is represented the increase in MTOW at the same condition. After a certain DoH no benefit can be achieved from using a hybrid-electric aircraft or there exists an optimum in the DoH. This is due to the fact that in this case more energy is required to transport the batteries than the energy stored in the batteries itself [80]. There is also a limit to the maximum achievable DoH for most battery specific energy/range combinations.

6   Systems & Structure

6.1 Turn-Around & Landing Gear

Due to the different type of energy sources by the hybrid aircrafts, a major challenge for the aviation industry is the reduction of turnaround times by 40% by 2050 using novel handling concepts [10]. The Cloudrider double-hybrid concept uses three multiple energy sources, which make the ground operations much more difficult. The battery charging mode in cruise enables to reduce the turn-around time, because no batteries are needed to be charged during the handling process. The two liquid energy sources must tank parallel. Nevertheless, to fulfil the requirements stated in EU-OPS 1.305 (FAR 121.570) [4], the aircraft can only be refueled, when the last passenger has left the aircraft. To solve this issue in the future the autonomous ground service equipments have a huge potential to reduce the number of ground incidents and ensure fast and reliable processes in the handling operations [8].

Another challenge is the supply and store of LNG at the airport. The LNG can be sourced from large-scale liquefaction facilities near the gas field [44] and distributed to the airport by rail or truck in an intermodal container [44]. The cost of the LNG storage was considered in the economic calculation in section 7.

The compatibility with the airport is a relevant question in the design of the landing gear. The ranways are classified by a pavement classification number (PCN) [81]; this number principally depends on the type and strength of the surface [81]. Accordingly, the aircrafts have also an aircraft classification number (ACN), which are also influenced by the landing gear design [81]. The requirement for safe operation at a given airport is that the ACN shall never exceed the PCN [81]. In order to reduce the ACN, the Cloudrider was equipped with an additional wheel pairs for the higher airport compatibility. However, it is a tradeoff between airport compatibility and the complexity of the landing gear [81].

6.2 Fuselage & Structure

The two-aisle wide body arrangement allows shorter boarding times, which is a crucial point in the reduction of airport turnaround times. As mentioned in the section 4, the lifting body arrangement has positive aerodynamic effects as well. Figure 11 introduces a possible 280 PAX arrangement, with a three class (first, comfort, economy) layout.
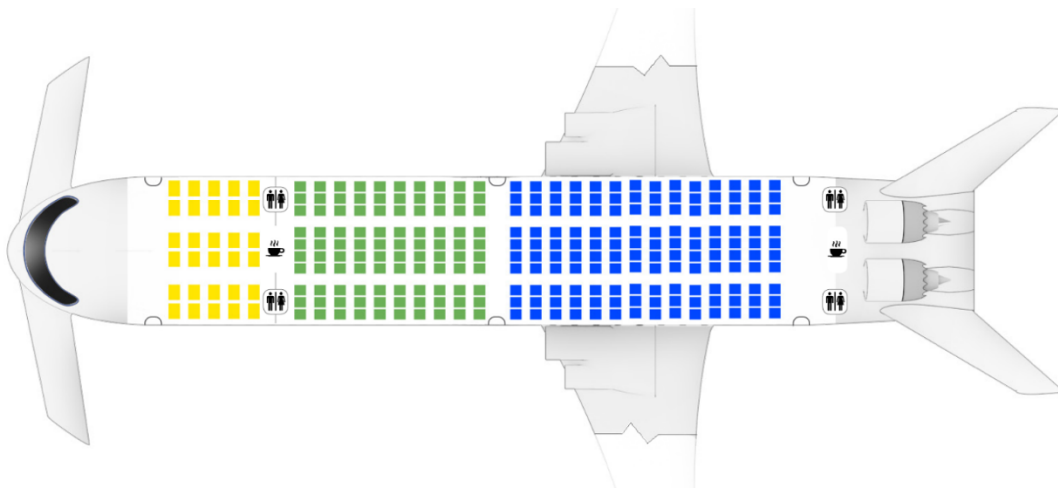

Figure 11: Twin-aisle, three class layout

The shown cabin layout is characterized by a double-bubble-like [82] cross section and accommodates 280 PAX in a triple class configuration with a 10 abreast seating arrangement in economy class and a 32 inch (0.813 m) seat pitch. The comfort class is equipped with 100 seats with 10 abreast

(and the business class has 12 seats with 4 abreast and a 36 inch (0.914 m) seat pitch. Passenger service areas, such as lavatories and galleys, can be found in the area of the for- ward and aft exit. In terms of ground handling interfaces, the Cloudrider is equipped with 6 passenger doors and 8 cargo doors. The six cargo doors are sized to accommodate LD3-45 containers Figure 12Figure 12:. The battery pack is laded in similar shaped boxes, and it is located more frontward to improve stability (this allows a smaller CG variation). Due to similar reasons, and to achieve a larger cargo place the LNG is stored in a twin container, before the wing. The application of the composite material technology allows a noticeable structural weights reduction. One interesting relevant future technology is the genetic algorithm strategy for optimization in an aircraft conceptual design, which may lead to a weight reduction at the components with constant load on the airplane [15].
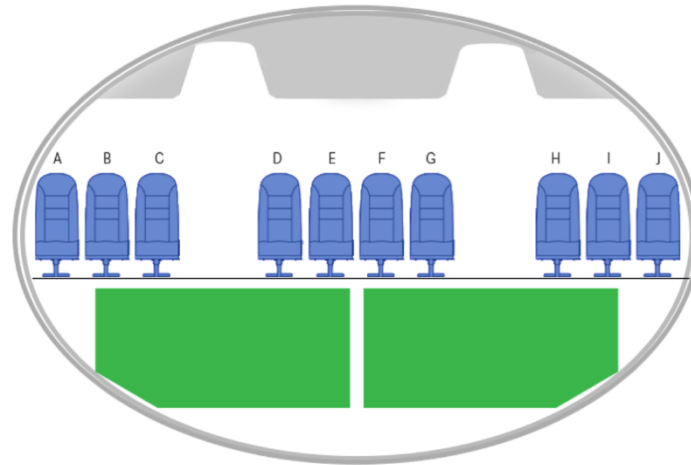

Figure 12: Fuselage cross section

7 Economic considerations

The aims of this analysis are to compare the Cash Operating Cost (COC) [83] of the Cloudrider Double-Hybrid concept to conventional aircrafts such as Airbus A330-200 and Boing 737-900ER and to specify the Cost-Specific Air Range (COSAR) and cost functions of the double-hybrid system which enable us to optimize and compare the flight profile according to time- and energy-related cost [10]. The four major differences of a conventional aircraft from the COC analysis are the following:

- Price of LNG and electricity compared to JET-A1 fuel
- Cost of fees with focus on Emission Trading System (ETS) Charge
- Depreciation costs of batteries for aeronautical applications
- Maintenance costs with focus on HTS motors and their sub-systems

We analyzed market history and projections for jet fuel, natural gas and electricity using data taken from the EIA [84] and EUROSTAT [85] database, in order to establish realistic assumptions about future prices. From Figure 13, it can be seen that LNG is currently one of the cheapest fuels available. The global reserves of natural gas are enormous, thus implying that the LNG price would be stable. However, there are additional costs associated with converting natural gas to LNG [6]. Storage of LNG at the airport requires specialized cryogenic holding tanks and handling equipment. A storage tank with enough capacity for 10 days of operations cost $1-3M. [6] The final at-pump price of LNG based on the EIA dates is estimated to be $11.29/MMBtu.
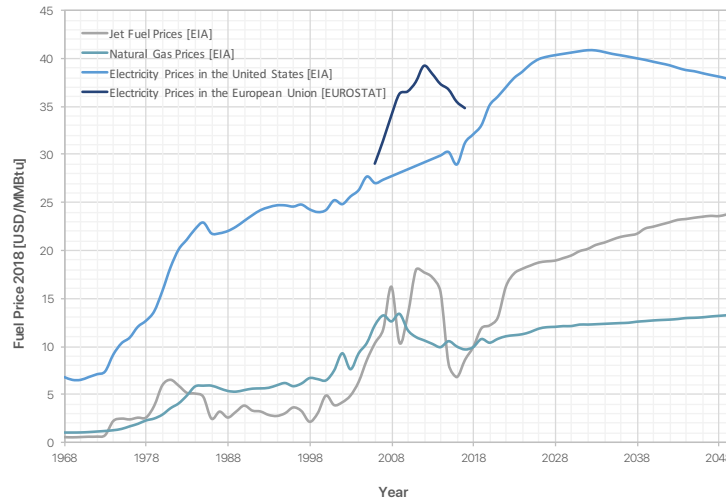
Figure 13.: Energy prices: history and projections (self made analysis from the EIA and EUROSTAT data)

The electricity prices vary greatly between different countries [86]; Figure 13 illustrate average values from the US and the EU. That electricity prices might be more than 30% higher compared to the prices of jet fuel and more than 50% higher compared to the natural gas prices. For operations in 2050, it is questionable if electricity prices will be completely independent from crude oil prices. Despite minor drops in fuel prices in recent years, EIA projections show that the general trend is expected to continue upwards [84], and based on these studies, we take a nominal price of $28/MMBtu for conventional jet fuel.

In the COC comparison to the Airbus A330-200 and Boeing 737-900ER the Cloudrider has higher fees for navigation, landing and ground operations because it has higher MTOW than the other baseline aircrafts. One more relevant cost parameter is the European Union Emission Trading System (EU ETS) is considered the flagship of the European Union's climate policies, and aircraft operators have been obliged to surrender allowances for their CO_2 emissions in the scope of EU ETS since 2012 [87]. The Double-Hybrid propulsion system of the Cloudrider reduces the CO_2 emission by about 56%, which enables significant savings in ETS Charges.

Maintenance Airframe & Systems costs are based on with OWE and flight cycles, which were assumed, from the data, statistical as 1200 cycles per year. This specification allows a remarkable reduction in the maintenance costs compared to the baseline aircrafts. An additional reason for the decrease in COC can be expected because of higher efficiency chains from the batteries to the HTS motor of the propulsive device. [54] Furthermore the LNG system reduces the energy consumption by 12% which leads to possible reductions in fuel/energy costs by around 12%, assuming congruity in prices for both types.

The depreciation costs of used batteries are critical for aircraft economics and they lead to an additional increase of COC by more than 35%. The estimation of COC was based on the method proposed by Torenbeek [16] and Direct Maintenance Costs (DMC) models were developed by Wessler [11]. All presented cost elements are shown in Figure 14. The novel aerodynamic and Double-Hybrid propulsion design enables significant savings in COC compared to the baseline concepts and using the assumptions of the cost methods.
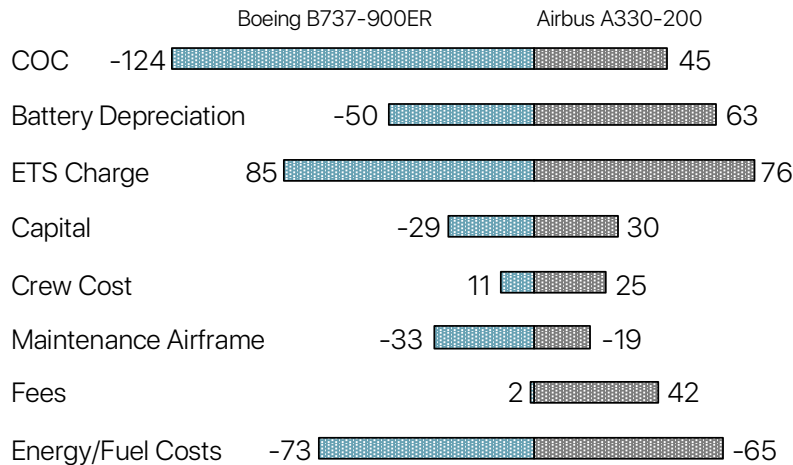
	Boeing B737-900ER	Airbus A330-200	
COC	-124		45
Battery Depreciation	-50		63
ETS Charge	85		76
Capital	-29		30
Crew Cost	11		25
Maintenance Airframe	-33		-19
Fees	2		42
Energy/Fuel Costs	-73		-65

Figure 14.: Cost comparison of the Cloudrider to the reference aircrafts

8 Conclusion

After an analysis of the future market and technology trends in the aviation industry, a comprehensive interdisciplinary aircraft design process for a non-conventional, ultra-efficient aircraft was introduced. This project is based around a pre-concept called the Cloudrider, which also complies with the new NASA N+3 [3] and European Commission Flightpath 2050 [4]requirements, especially focusing on energy reduction and alternative propulsion and energy systems.
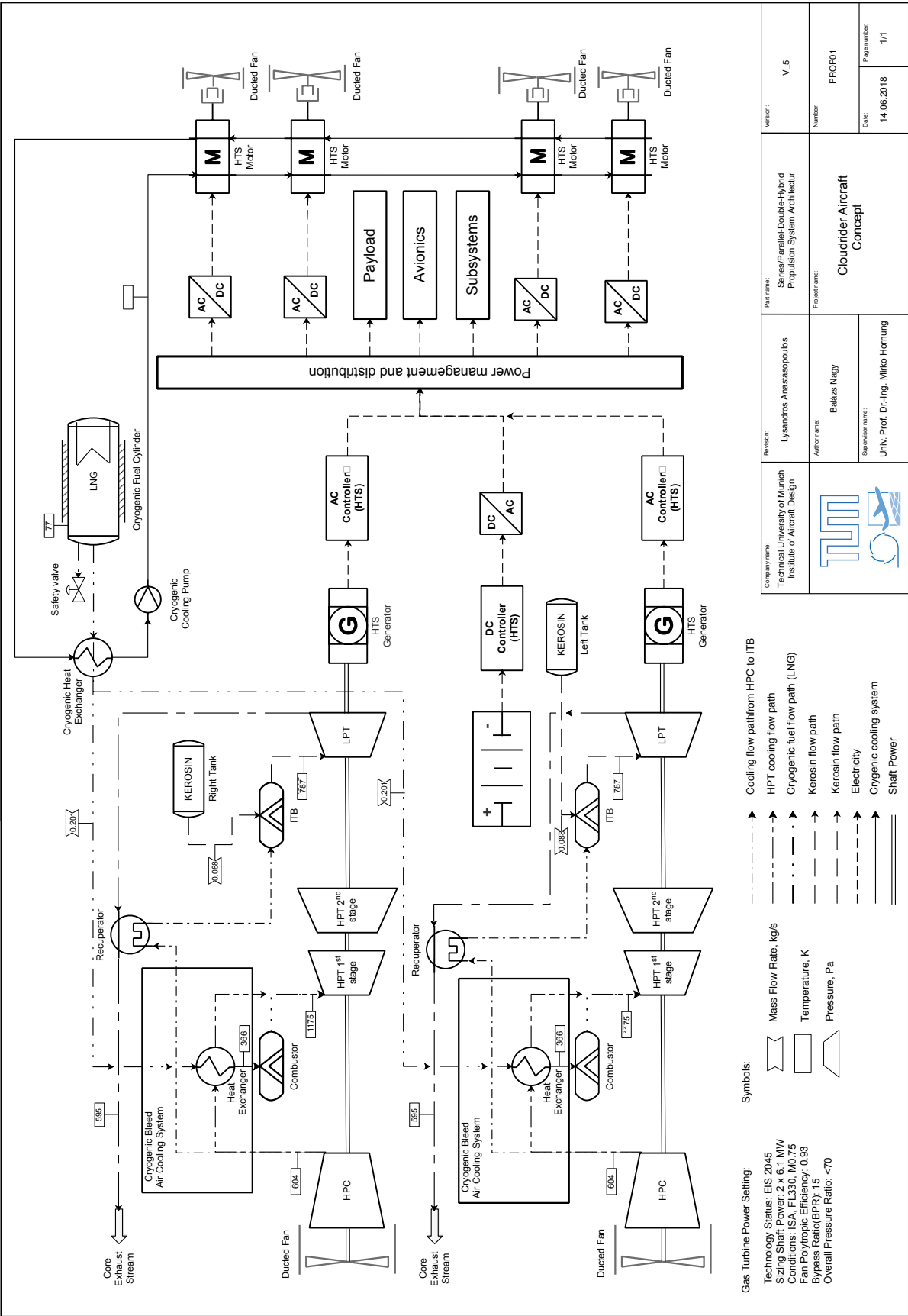
In this design study, within the scope of the Aircraft Design Challenge of NASA and DLR was created a unique airframe and a novel propulsion system design researched, investigated and implemented, in order to fulfil the strict requirements for future aircraft design. The four main parts of the design process were the analysis of the market demand, aerodynamics, propulsion system and the investigation of feasibility with the help of comparison with the baseline aircraft.

The aerodynamic design of the Cloudrider concept has a semi conventional, three lifting surface, with a promising total wetted area reduction potential. To maximize the aerodynamic efficiency, high aspect ratio wings are deployed, equipped with hybrid laminar flow control (HLFC) devices.

The non-regular hybrid-distributed-propulsion system with three different energy sources (LNG, kerosene and batteries) had caused many design challenges during the sizing process and also a novel handling process was necessary. These challenges include, among others the engine optimization, which was conducted in the flexible modeling environment CycleTempo®. To achieve the prescribed energy reduction the operating mode of the gas turbine and the batteries was also investigated and simulated based on the in-house developed model implemented in Wolfram Mathematica®. In addition, with regards to motive power the proposal utilizes ducted fans run by High-Temperature Super-conducting (HTS) electric motors, using the heat of the LNG as a cryogenic cooling system.

The resulting optimized propulsion system combined with the novel airframe design of the Cloudrider concept has achieved 85% in total LTO NOx and 60.6% reduction in energy in payload km compared to the Boeing B737-900ER baseline aircraft.

9 Appendix

Ducted Fan

HTS Motor · M (×4)

AC / DC (×4)

Payload

Avionics

Subsystems

Power management and distribution

LNG

Cryogenic Fuel Cylinder

Safety valve

Cryogenic Cooling Pump

Cryogenic Heat Exchanger

77

AC Controller (HTS)

DC Controller (HTS)

DC / AC

AC Controller (HTS)

HTS Generator · G

KEROSIN Left Tank

KEROSIN Right Tank

LPT

ITB · 787

HPT 2nd stage

HPT 1st stage

1175

366

Heat Exchanger

Combustor

604

HPC

Recuperator

Cryogenic Bleed Air Cooling System

595

Core Exhaust Stream

Ducted Fan

0.088

0.20

HTS Generator · G

1175

117.5

Gas Turbine Power Setting:

Technology Status: EIS 2045
Sizing Shaft Power: 2 x 6.1 MW
Conditions: ISA, FL330, M0.75
Fan Polytropic Efficiency: 0.93
Bypass Ratio (BPR): 15
Overall Pressure Ratio: <70

Symbols:

⊳◁ Mass Flow Rate, kg/s

▢ Temperature, K

⬡ Pressure, Pa

Cooling flow path from HPC to ITB
HPT cooling flow path
Cryogenic fuel flow path (LNG)
Kerosin flow path
Kerosin flow path
Electricity
Cryogenic cooling system
Shaft Power

Company name:	Revision:	Part name:	Version:
Technical University of Munich, Institute of Aircraft Design	Lysandros Anastasopoulos	Series/Parallel-Double-Hybrid Propulsion System Architecture	V_5

Author name:	Project name:	Number:
Balázs Nagy	Cloudrider Aircraft Concept	PROP01

Supervisor name: Univ.-Prof. Dr.-Ing. Mirko Hornung

Date: 14.06.2018 Page number: 1/1

10 References

[1] *http://www.iata.org/pressroom/pr/Pages/2016-10-18-02.aspx*.

[2] Nateri Madavan, *A NASA Perspective on Electric Propulsion Technologies for Future Generations of Large Commercial Aircraft*.

[3] John M. Morgenstern, Nicole Norstrud, and Dr. Marc Stelmack: *Advanced Concept Studies for Supersonic Commercial Transports Entering Service in 2030-35 (N+3)*.

[4] *Flightpath 2050: Europe's vision for aviation*. Luxembourg: Office for Official Publications of the European Communities, 2011.

[5] M. Schmidt, A. Paul, M. Cole, and K. O. Ploetner, "Challenges for ground operations arising from aircraft concepts using alternative energy," *Journal of Air Transport Management*, vol. 56, pp. 107–117, 2016.

[6] E. M. Greitzer *et al., N+3 Aircraft Concept Designs and Trade Studies. Volume 1*.

[7] Alessandro Sgueglia *et al., Exploration and Sizing of a Large Passenger Aircraft with Distributed Ducted Electric Fans*.

[8] Arne Seitz, Oliver Schmitz, Askin T. Isikveren, and Mirko Hornung, *Electrically powered Propulsion: Comparsion and Contrast To Gas Turbines*.

[9] Askin T. Isikveren *et al., Conceptual Studies Of Universally-Electric Systems Architectures Suitable For Transport Aircraft*. Munich, Germany.

[10] C. Pornet, S. Kaiser, and C. Gologan, *Cost-based flight technique optimization for hybrid energy aircraft*.

[11] H. Pfaender, *Fuel Consumption, FAA US Operations Data Analysis*.

[12] *Avanti P180 II Specification and Description*.

[13] *Short/medium-haul widebody airliner market*.

[14] D. P. Raymer, *Aircraft design: A conceptual approach,* 2nd ed. Washington, D.C.: AIAA, 1992.

[15] M. Jahanmiri, *Aircraft Drag Reduction: An Overview: A review on aicraft drag reduction methods,* 1st ed. Saarbrücken: LAP LAMBERT Academic Publishing, 2013.

[16] E. Torenbeek, *Advanced aircraft design: Conceptual design, analysis, and optimization of subsonic civil airplanes / Egbert Torenbeek, Delft University of Technology, The Netherlands*. Chichester, West Sussex, United Kingdom: Wiley, 2013.

[17] A. FREDIANI, V. CIPOLLA, K. ABU SALEM, V. BINANTE, and M. PICCHI SCARDAONI, "On the preliminary design of PrandtlPlane civil transport aircraft," (Eng), 2017.

[18] T. A. Reist and D. W. Zingg, *Aerodynamic Design of Blended Wing-Body and Lifting-Fuselage Aircraft*.

[19] S. Gudmundsson, *General aviation aircraft design: Applied methods and procedures*. Oxford, UK: Butterworth-Heinemann, 221E2014.

[20] M. S. Selig, M. D. Maughmert, and D. M. Somers, *Natural-Laminar-Flow Airfoil for General-Aviation Applications*.

[21] D. M. Somers, *Design of a Slotted, Natural-Laminar-Flow Airfoil for Business-Jet Applications*.

[22] *Technical status review on drag prediction and analysis fromcomputational fluid dynamics: State of the art*. Neuilly sur Seine: North Atlantic Treaty Organization, AdvisoryGroup for Aerospace Research and Development, 1989.

[23] N. N. Gavrilović, B. P. Rašuo, G. S. Dulikravich, and V. B. Parezanović, *Commercial Aircraft Performance Improvement Using Winglets*.

[24] L. Prandtl, *Über Targflügel kleinsten induzierten Widerstandes*.

[25] Bowers *et al., On Wings of the Minimum Induced Drag: Spanload Implications for Aircraft and Birds*.

[26] K. ROKHSAZ and B. P. SELBERG, "Three-surface aircraft - Optimum vs typical," *Journal of Aircraft*, vol. 26, no. 8, pp. 699–704, 1989.

[27] J. D. Phillips, *Approximate neutral point of a subsonic canard aircraft*.

[28] D. Strohmeyer, W. Heinze, C. Österheld, and L. Fornaister, *Three Surface Aircraft -A Concept for Future Transport Aircraft*.

[29] M. Hornung, *Flugzeugentwurf*.

[30] S.-H. Ko, J.-S. Bae, and J.-H. Rho, "Development of a morphing flap using shape memory alloy actuators: the aerodynamic characteristics of a morphing flap," *Smart Mater. Struct.*, vol. 23, no. 7, p. 74015, 2014.

[31] Y. Yadlin and A. Shmilovich, "Lift Enhancement for Upper Surface Blowing Airplanes," in *31st AIAA Applied Aerodynamics Conference*, San Diego, CA, 06242013, p. 1354.

[32] J. Roskam, *Airplane design*. Lawrence (Kansas): DARcorporation, 2004-2011.

[33] Rudi Kirner, "An Investigation into the Benefits of Distributed Propulsion on Advanced Aircraft Configurations," PhD, CRANFIELD UNIVERSITY, 2013.

[34] Andy Ko, J.A. Schetz, and William H. Mason, *Assessment of the Potential Advantages of Distributed-Propulsion for Aircraft*.

[35] Alex M. Stoll, JoeBen Bevirt, Mark D. Moore William J. Fredericks, and Nicholas K. Bore, *Drag Reduction Through Distributed Electric Propulsion*.

[36] A. G. Rolls-Royce, *E-THRUST Electrical distributed propulsion system concept for lower fuel consumption, fewer emissions and less noise*.

[37] A. S. Gohardani, G. Doulgeris, and R. Singh, "Challenges of future aircraft propulsion: A review of distributed propulsion technology and its potential application for the all electric commercial aircraft," *Progress in Aerospace Sciences*, vol. 47, no. 5, pp. 369–391, 2011.

[38] Hans-Jörg Steiner, Patrick C. Vratny, Corin Gologan, and Kerstin Wieczorek, *Performance and Sizing of Transport Aircraft Employing Electrically-Powered Distributed Propulsion*.

[39] A. T. Isikveren, *The Method of Quadrant Based Algorithmic Nomographs for Hybrid/Electric Aircraft Pre-design*.

[40] R. A. Roberts, S. R. Nuzum, and M. Wolff, "Liquefied Natural Gas as the Next Aviation Fuel," in *13th International Energy Conversion Engineering Conference*, Orlando, FL, 07272015, p. 1071.

[41] H. Kuhn, A. Seitz, L. Lorenz, Isikveren A.T., and A. Sizmann, *Progress And Perspectives Of Electric Air Transport*.

[42] K. C. Bilashm, *Electric Vehicle Batteries: Li-ion and Beyond, Challenges and Advancements*.

[43] K. Rajashekara, "Present Status and Future Trends in Electric Vehicle Propulsion Technologies," *IEEE J. Emerg. Sel. Topics Power Electron.*, vol. 1, no. 1, pp. 3–10, 2013.

[44] M. R. Withers *et al.,* "Economic and environmental assessment of liquefied natural gas as a supplemental aircraft fuel," *Progress in Aerospace Sciences*, vol. 66, pp. 17–36, 2014.

[45] M. K. Bradley and C. K. Droney, *Subsonic Ultra Green Aircraft Research*.

[46] https://www.technologyreview.com/s/516576/once-a-joke-battery-powered-airplanes-are-nearing-reality/.

[47] S. Kumar, S. Suresh, and S. Arisutha, "Production of Renewable Natural Gas from Waste Biomass," *J. Inst. Eng. India Ser. E*, vol. 94, no. 1, pp. 55–59, 2013.

[48] https://www.afdc.energy.gov/fuels/natural_gas_renewable.html.

[49] U.S. Energy information administration, *Annual energy outlook 2012*.

[50] L.K. Carson, G.W. Davis, E.F. Versaw, G .R. Cunnington, JR., and E.J. Daniels, *Study of Methane Fuel For Subsonic Transport Aircraft*.

[51] Marty K. Bradley and Christopher K. Droney, *Subsonic Ultra Green Aircraft Research Phase?ll: N+4 Advanced Concept Development*.

[52] K. T. Chau and Y. S. Wong, *Overview of power management in hybrid electric vehicles*.

[53] C. Pornet and A. T. Isikveren, "Conceptual design of hybrid-electric transport aircraft," *Progress in Aerospace Sciences*, vol. 79, pp. 114–135, 2015.

[54] Cesar A. Luongo *et al., Next Generation More-Electric Aircraft: A Potential Application for HTS Superconductors*.

[55] F. Berg, J. Palmer, L. Bertola, P. Miller, and G. Dodds, "Cryogenic system options for a superconducting aircraft propulsion system," *IOP Conf. Ser.: Mater. Sci. Eng.*, vol. 101, p. 12085, 2015.

[56] P. Dai *et al., Synthesis and neutron powder diffraction study of the superconductor HgBa2Ca2Cu3O8+d by T1 substitution*.

[57] Jules E. Pienkos, Philippe J. Masson, Sastry V. Pamidi, and Cesar A. Luongo, *Conduction Cooling of a Compact HTS Motor for Aeropropulsion*.

[58] *https://eur-lex.europa.eu/legal-content/EN/ALL/?uri=celex%3A32008R0859*.

[59] *https://www.easa.europa.eu/certification-specifications/cs-25-large-aeroplanes*.

[60] C. Pornet *et al.,* "Methodology for Sizing and Performance Assessment of Hybrid Energy Aircraft," *Journal of Aircraft*, vol. 52, no. 1, pp. 341–352, 2015.

[61] Arthur V. Radun, *Design Considerations for the Switched Reluctance Motor*.

[62] *http://reference.wolfram.com/language/guide/HelpMenu.html*.

[63] *http://www.asimptote.nl/software/cycle-tempo/*.

[64] A. Seitz, A. T. Isikveren, and M. Hornung, "Pre-Concept Performance Investigation of Electrically Powered Aero-Propulsion Systems," in *49th AIAA/ASME/SAE/ASEE Joint Propulsion Conference*, San Jose, CA, 07142013, p. 748.

[65] M. C. Schwarze and T. Zold, *Angepasste Flugzeugkonfigurationen Für Die Energieeficiente Open-Rotor Integration Auf Zukünftigen Kurzstrecken-Verkehrsflugzeugen*.

[66] A. T. Isikveren, A. Seitz, P. C. Vratny, and C. Pornet, *Conceptual Studies of Universally-Electric Systems Architectures Suitable for Transport Aircraft*.

[67] F. Yin, A. Gangoli Rao, A. Bhat, and M. Chen, "Performance assessment of a multi-fuel hybrid engine for future aircraft," *Aerospace Science and Technology*, vol. 77, pp. 217–227, 2018.

[68] P. Callewaert *et al., Multifuel Blended Wing Body Delft University of Technology*.

[69] F. Joos, P. Brunner, Schulte-Werning B., K. Syed, and A. Eroglu, *DEVELOPMENT OF THE SEQUENTIAL COMBUSTION SYSTEM FOR THE ABB GT24/GT26 GAS TURBINE FAMILY*.

[70] *https://www.compositesworld.com/blog/post/the-next-generation-of-ceramic-matrix-composites*.

[71] *http://www.boeing.com/assets/pdf/commercial/airports/acaps/737.pdf*.

[72] *http://www.airbus.com/aircraft/support-services/airport-operations-and-technical-data/aircraft-characteristics.html*.

[73] L. Sanders *et al.,* "Prediction of the acoustic shielding by aircraft empennage for contra-rotating open rotors," *International Journal of Aeroacoustics*, vol. 16, no. 7-8, pp. 626–648, 2017.

[74] *https://www2.lba.de/data/bb/Motoren/en_6329_00.pdf*.

[75] L. Larsson, T. Gönstedt, and K. G. Kyprianidis, *Conceptual Design And Mission Analysis For A Geared Turbofan And An Open Rotor Configuration*.

[76] G. Yueping and H. T. Russel, *Experimental Study on Open Rotor Noise Shielding by Hybrid-Wing-Body Aircraft*.

[77] Dale E. Van Zante, *The NASA Environmentally Responsible Aviation Project/General Electric Open Rotor Test Campaign*.

[78] M. D. Guynn, J. J. Berton, W. J. Haller, E. S. Hendricks, and M. T. Tong, *Performance and Environmental Assessment of an Advanced Aircraft with Open Rotor Propulsion*.

[79] *ICAO Database*.

[80] M. Voskuijl, J. van Bogaert, and A. G. Rao, "Analysis and design of hybrid electric regional turboprop aircraft," *CEAS Aeronaut J*, vol. 9, no. 1, pp. 15–25, 2018.

[81] R. Henke, T. Lammering, and E. Anton, *Impact of an Innovative Quiet Regional Aircraft on the Air Transportation System*.

[82] M. Drela, *Development of the D8 Transport Configuration*.

[83] *http://ceras.ilr.rwth-aachen.de/*.

[84] *https://www.eia.gov/petroleum/reports.php#/T1288*.

[85] *http://ec.europa.eu/eurostat/news/themes-in-the-spotlight/energy-prices*.

[86] *https://www.statista.com/statistics/263492/electricity-prices-in-selected-countries/*.

[87] PwC, *ETS Aviation small emitters*.

Team Members:

Balázs Nagy, BSc.

Master student in Energy- and Process Engineering, 2nd Semester

Focus on Propulsion System

E-mail: balazs.nagy@tum.de

Soma Detre, BSc.

Master student in Aerospace Engineering, 5th semester

Focus on Aerodynamics and CAD Structure

E-mail: ga85jus@tum.de

Technische Universität München

Fakultät für Maschinenwesen
Institut für Luft- & Raumfahrt
Lehrstuhl für Luftfahrtsysteme

Prof. Dr.-Ing.
Mirko Hornung

Boltzmannstraße 15
85748 Garching bei München

Tel   +49.89.289.15981
Fax   +49.89.289.15982

sekretariat@lls.mw.tum.de
www.lls.mw.tum.de

Technische Universität München . Lehrstuhl für Luftfahrtsysteme
Boltzmannstraße 15 . 85748 Garching . Germany
Lehrstuhl für Luftfahrtsysteme
Institut für Luft- und Raumfahrt
Boltzmannstraße 15
85748 Garching b. München

Garching, 19. Juni 2018

Bestätigungsschreiben

Sehr geehrte Damen und Herren,

mit diesem Schreiben wird bescheinigt, dass der Beitrag der Studierenden zum studentischen Wettbewerb *DLR-NASA-Challenge 2018* am Lehrstuhl für Luftfahrtsysteme geprüft und genehmigt wurde. Die Einreichung der Berichte wird damit befürwortet.

Bei weiteren Fragen können Sie sich gerne an mich oder den betreuenden Mitarbeiter Herrn Lysandros Anastasopoulos (lysandros.anastasopoulos@tum.de) wenden.

Mit freundlichen Grüßen

Univ. Prof. Dr.-Ing. Mirko Hornung
Ordinarius des Lehrstuhls für Luftfahrtsysteme

Technische Universität München

Fakultät für Maschinenwesen
Institut für Luft- & Raumfahrt
Lehrstuhl für Luftfahrtsysteme

Prof. Dr.-Ing.
Mirko Hornung

Boltzmannstraße 15
85748 Garching
Germany

Tel   +49.89.289.15981
Fax   +49.89.289.15982

sekretariat@lls.mw.tum.de
www.lls.mw.tum.de

Technische Universität München . Lehrstuhl für Luftfahrtsysteme
Boltzmannstraße 15 . 85748 Garching . Germany

Lehrstuhl für Luftfahrtsysteme
Institut für Luft- und Raumfahrt
Boltzmannstraße 15
85748 Garching

Garching, 29.06.2018

Bestätigungsschreiben

Sehr geehrte Damen und Herren,

hiermit bestätige ich, dass die Mitglieder der studentischen Arbeitsgruppe (LLS-Team 2):

- Soma Detre
- Balázs Nagy

die Arbeit zum Wettbewerb DLR-NASA-Challenge 2018 eigenständig angefertigt haben.

Bei weiteren Fragen können Sie sich gerne an mich oder den betreuenden Mitarbeiter Herrn Lysandros Anastasopoulos (Email: lysandros.anastasopoulos@tum.de) wenden.

Mit freundlichen Grüßen

Christian Rößler
Akad. Rat des Lehrstuhls für Luftfahrtsysteme